

See discussions, stats, and author profiles for this publication at: <https://www.researchgate.net/publication/259935222>

Design, Synthesis and Structure–Activity Relationship of Novel

DATASET · JANUARY 2014

CITATIONS

2

READS

65

11 AUTHORS, INCLUDING:



[Gerhard Wolber](#)

Freie Universität Berlin

145 PUBLICATIONS **2,764** CITATIONS

[SEE PROFILE](#)



[Hoda El Diwani](#)

National Research Center, Egypt

39 PUBLICATIONS **542** CITATIONS

[SEE PROFILE](#)

Accepted Manuscript

Design, Synthesis and Structure-Activity Relationship of Novel Quinoxaline Derivatives as Cancer Chemopreventive Agent by Inhibition of Tyrosine Kinase Receptor

Shadia A. Galal, Ahmed S. Abdelsamie, Salwa M. Soliman, Jeremie Mortier, Gerhard Wolber, Mamdouh M. Ali, Harukuni Tokuda, Nobutaka Suzuki, Akira Lida, Raghda A. Ramadan, Hoda I. El Diwani

PII: S0223-5234(13)00502-3

DOI: [10.1016/j.ejmech.2013.07.049](https://doi.org/10.1016/j.ejmech.2013.07.049)

Reference: EJMECH 6341

To appear in: *European Journal of Medicinal Chemistry*

Received Date: 13 May 2013

Revised Date: 28 July 2013

Accepted Date: 30 July 2013

Please cite this article as: S.A. Galal, A.S. Abdelsamie, S.M. Soliman, J. Mortier, G. Wolber, M.M. Ali, H. Tokuda, N. Suzuki, A. Lida, R.A. Ramadan, H.I. El Diwani, Design, Synthesis and Structure-Activity Relationship of Novel Quinoxaline Derivatives as Cancer Chemopreventive Agent by Inhibition of Tyrosine Kinase Receptor, *European Journal of Medicinal Chemistry* (2013), doi: 10.1016/j.ejmech.2013.07.049.

This is a PDF file of an unedited manuscript that has been accepted for publication. As a service to our customers we are providing this early version of the manuscript. The manuscript will undergo copyediting, typesetting, and review of the resulting proof before it is published in its final form. Please note that during the production process errors may be discovered which could affect the content, and all legal disclaimers that apply to the journal pertain.



Design, Synthesis and Structure-Activity Relationship of Novel Quinoxaline Derivatives as Cancer Chemopreventive Agent by Inhibition of Tyrosine Kinase Receptor

Shadia A. Galal^{a,*}, Ahmed S. Abdelsamie^a, Salwa M. Soliman^b, Jeremie Mortier^{b,c}, Gerhard Wolber^b, Mamdouh M. Ali^d, Harukuni Tokuda^e, Nobutaka Suzuki^e, Akira Lida^f, Raghda A. Ramadan^g, and Hoda I. El Diwani^a

^a: Department of Chemistry of Natural and Microbial Products, Division of Pharmaceutical and Drug Industries, National Research Center, Dokki, 12622, Cairo, Egypt.

^b: Department of Pharmaceutical Chemistry, Institute of Pharmacy, Freie Universitaet Berlin, Koenigin Luise Strasse, Berlin 14195, Germany.

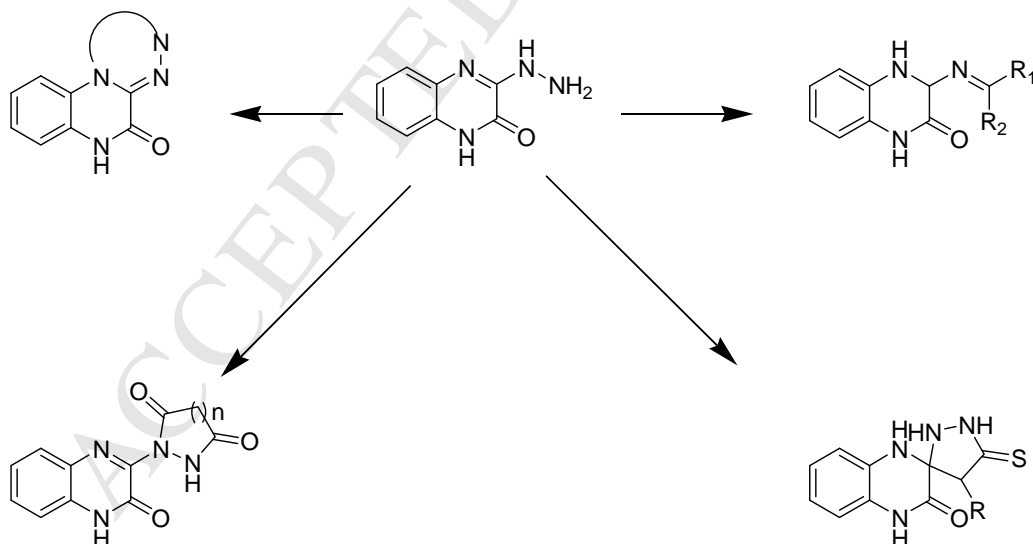
^c: Department of Organic Chemistry, Free University Berlin, Takustraße 3, D-14195 Berlin, Germany.

^d: Department Biochemistry, Division of Genetic Engineering and Biotechnology, National Research Centre, , Dokki, 12622, Cairo, Egypt.

^e: Department of Complementary and Alternative Medicine, R&D, Graduate School of Medical Science, Kanazawa University, 13-1 Takara-machi, Kanazawa, Japan

^f: Faculty of Agriculture, Kinki University, 3327-20 Naka-machi, Nara, JAPAN 631-8505

^g: Youssef Jameel Science and Technology Research Center, The American University in Cairo, New Cairo, Egypt



The protein tyrosine kinase inhibition and molecular docking studies of new quinoxaline derivatives were performed in order to rationalize their studied chemopreventive activity.

Design, Synthesis and Structure-Activity Relationship of Novel Quinoxaline Derivatives as Cancer Chemopreventive Agent by Inhibition of Tyrosine Kinase Receptor

Shadia A. Galal^{a*}, Ahmed S. Abdelsamie^a, Salwa M. Soliman^b, Jeremie Mortier^{b,c}, Gerhard Wolber^b, Mamdouh M. Ali^d, Harukuni Tokuda^e, Nobutaka Suzuki^e, Akira Lida^f, Raghda A. Ramadan^g, and Hoda I. El Diwani^a

^a: Department of Chemistry of Natural and Microbial Products, Division of Pharmaceutical and Drug Industries, National Research Center, Dokki, 12622, Cairo, Egypt.

^b: Department of Pharmaceutical Chemistry, Institute of Pharmacy, Freie Universitaet Berlin, Koenigin Luise Strasse, Berlin 14195, Germany.

^c: Department of Organic Chemistry, Free University Berlin, Takustraße 3, D-14195 Berlin, Germany.

^d:Department Biochemistry, Division of Genetic Engineering and Biotechnology, National Research Centre, , Dokki, 12622, Cairo, Egypt.

^e: Department of Complementary and Alternative Medicine, R&D, Graduate School of Medical Science, Kanazawa University,13-1 Takara-machi, Kanazawa, Japan

^f:Faculty of Agriculture, Kinki University, 3327-20 Naka-machi, Nara, JAPAN 631-8505

^g: Youssef Jameel Science and Technology Research Center, The American University in Cairo, New Cairo, Egypt.

Abstract

The cancer chemopreventive activity of quinoxaline derivatives **1-20** has been evaluated by studying the inhibitory effect on Epstein–Barr virus early antigen (EBV-EA) activation. The quinoxaline derivatives **1-20** showed inhibitory effect on EBV-EA activation without cytotoxicity on Raji cells. All compounds exhibited dose dependent inhibitory activities, most of them showed significant activity at 1000 mol ratio/12-*O*-tetradecanoylphorbol-13-acetate (TPA). Compounds **7** and **9** exhibited stronger inhibitory effects on the EBV-EA activation than that of the representative control, oleanolic acid, at the highest measured concentration. In addition, compounds **7-10** showed potent and selective inhibition of human tyrosine kinase (TRK) in liver cancer HepG2 and breast cancer MCF-7 cell lines similar to the positive control, doxorubicin.

*Corresponding author: E-mail: sh12galal@yahoo.com

Keywords

Synthesis; Quinoxalines; Epstein–Barr virus; Cancer chemopreventive activity; Docking; Protein tyrosine kinase .

1. Introduction

The wide spectrum of biological activities including antitumor activity of quinoxaline derivatives is known and well documented in the literature [1-10]. The activity of quinoxalines as antitumor agents may be due their ability of inhabitation of protein tyrosine kinases as c-kit enzyme [11,12]. C-kit is a member of the family protein tyrosine kinase III. Kinases are the key in cell signaling pathways that regulate cell growth, proliferation, and apoptosis. Consequently, unregulated kinase activity can result in uncontrolled cellular growth and inappropriate regulation of apoptosis; a key mechanism in oncogenesis. Quinoxalines are known to display a good affinity to the ATP-binding site of c-kit tyrosine protein [13-17].

On the other hand, the Epstein-Barr virus (EBV), also called human herpes virus 4 (HHV-4), is a cancer-causing virus of the herpes family which includes herpes simplex virus and cytomegalovirus. On infecting the *B*-lymphocyte, the linear virus genome circularizes and the virus subsequently persists within the cell as an episome. It is also known to cause several lymphoproliferative disorders and cancers, particularly Hodgkin's disease, Burkitt's lymphoma, nasopharyngeal carcinoma, and central nervous system lymphomas associated with HIV [18].

As a continuation to our previous work in discovering potent cancer chemopreventive agents, the aim of the present investigation was the synthesis of new hydrazinylquinoxalinones as analogues to compound **I** (c.f. Figure 1) that showed a relative ratio of inhibition of 9.2 with respect to TPA (100%) at the concentration of 1000mol ratio/TPA [19]. The activity of the new compounds was evaluated by studying the inhibitory effect on Epstein–Barr virus early antigen (EBV-EA) activation induced by 12-*O*-tetradecanoylphorbol-13-acetate (TPA), which stimulates cell proliferation through rapid activation of protein kinase C (PKC), followed by gradual degradation of the kinase [20].

2. Results and discussion

2.1. Chemistry

Quinoxalin-2,3(*1H,4H*)-dione (**1**) was synthesized by the method of Obafemi and Pfeiferer [21]. Stirring of compound **1** with phosphorus oxychloride in methylene chloride at room temperature gave 3-chloroquinoxalin-2(*1H*)-one (**2**) [19]. The X-ray structure of compound **2** was performed. (c.f. **Figure 2**). Crystal data, fractional atomic coordinates and equivalent isotropic thermal parameters, anisotropic displacement parameters and geometric parameters of **2** are given in supplementary data [22-25].

3-Hydrazinylquinoxalin-2(*1H*)-one (**3**) [26, 27] can be obtained by reaction of compound **1** or **2** with hydrazine hydrate in ethanol (c.f. Scheme 1). Hydrazones, especially the ones containing the azomethine ($-\text{NHN}=\text{CH}-$) protons, have been reported to possess anticancer activity [28, 29] and constitute an important class of compounds for new drug development [30, 31]. Scheme 2 was performed to produce the target hydrazones.

Treatment of compound (**3**) with acetone, *N,N*-dimethylaminobenzaldehyde or 2,6-dimethoxybenzaldehyde in ethanol yielded hydrazinylquinoxalinones as 3-(2-(propan-2-ylidene)hydrazinyl)quinoxalin-2(*1H*)-one (**4**) [32], 3-(2-(4-(dimethylamino)benzylidene)hydrazinyl)quinoxalin-2(*1H*)-one (**5**) and 3-(2-(2,6-dimethoxybenzylidene)hydrazinyl)quinoxalin-2(*1H*)-one (**6**), respectively, (c.f. Scheme 2). Treatment of compounds **5** or **6** with equimolar amount of allyl bromide or ethyl chloroacetate yielded selectively the 1-alkylated products **7-10** respectively (c.f. Scheme 2). This was indicated by the disappearance of NH of quinoxaline in compounds **7-10** in both IR and ^1H -NMR spectra with respect to compound **5** and **6**. Also, the significant lower frequency shift of $\nu(\text{C}=\text{O})$ from 1687 cm^{-1} in compound **5** to 1646 cm^{-1} in compound **7** and to 1647 cm^{-1} in compound **8** was observed. In compounds **9** and **10**, the $\nu(\text{C}=\text{O})$ signals appeared at 1649 cm^{-1} and 1637 cm^{-1} respectively with remarkable lower frequency shift with respect to compound **6** (1694 cm^{-1}). The significant frequency shifts in C=O moiety in IR in addition to the disappearance of NH bands of quinoxaline moiety in IR and ^1H -NMR spectra of compounds **7-10** proved that alkylation took place selectively at position 1.

As was known from the literature, annelation in heterocyclic-fused quinoxalines was successful in causing selectivity and strong affinity towards the receptor [5,6,19]. Prompted by the previous findings, annelated quinoxalines were synthesized through scheme 3. 3-Hydrazinylquinoxalin-2(1*H*)-one (**3**) was used as starting agent to prepare triazino[4,3-*a*]quinoxaline derivatives (**11-14**) and triazolo[4,3-*a*]quinoxaline (**15, 16**) by treating compound **3** with ethyl bromoacetate, chloroacetyl chloride, ethyl oxamate, diethyl oxalate, ethyl chloroformate and triethyl orthoformate, respectively. (c.f. scheme 3).

Spiroquinoxalines were prepared to observe the effect of such structure on activity. Reactions of methyl isothiocyanate or benzoyl isothiocyanate with 3-hydrazinylquinoxalin-2(1*H*)-one (**3**) were investigated and gave the 5'-thioxo-1*H*-spiro[quinoxaline-2,3'-[1,2,4]triazolidin]-3(4*H*)-one derivatives (**17,18**) (Scheme 4). The structure of compounds **17, 18** was deduced from their elemental analyses, IR, and ¹H NMR data. Their mass spectra displayed molecular ion peaks at appropriate *m/z* values. The formation of spiro compounds could be explained by the mechanism involving the imine carbon atom of quinoxaline in the reaction, with the nitrogen becoming electron-donating amine nitrogen. The formation of spiro-compounds was decidedly confirmed previously by single-crystal X-ray analyses by Mamedov et al [33].

Treatment of compound **3** with diethyl malonate or diethyl succinate in dimethyl formamide yielded quinoxaliny pyrazolidine derivative (**19**) and quinoxalinytetrahydro pyridazine derivative (**20**) respectively (c.f. Scheme 5).

2.2. Inhibition of EBV-EA activation assay

A primary screening test was carried out using a short-term *in vitro* synergistic assay on EBV-EA activation [34-36]. The inhibitory effect of quinoxaline derivatives **1-20** on the EBV-EA activation induced by TPA and the associated viability of Raji cells was listed in Table 1. In this assay, all the tested compounds showed inhibitory effects on EBV-EA activation and no cytotoxicity on Raji cells. All compounds exhibited dose dependent inhibitory activities, and the viability percentages of Raji cells treated with the tested compounds (**1-20**) were 50, 60 or 70% at the highest concentration of 1000 mol ratio/TPA. As shown in Table 1, at concentration 1000 mol ratio/TPA the inhibitory activity of compounds **7** and **9** were stronger than that of oleanolic acid, known as a

representative anti-tumor promoting agent [37]. Compound **8** had comparative activity with oleanolic acid. The relative ratio of inhibition of compound **7** with respect to TPA (100%) was 10.0, 41.6, 73.2, 100 % at the concentrations of 1000, 500, 100 and 10 mol ratio/TPA, respectively (Table 1); meaning 90.0, 58.4, 26.8 and 0.0% inhibition of the EBV-EA activation by TPA respectively. Compounds **9** and **8** showed 89.2, 58.0, 26.5 and 0%; and 87.3, 52.4, 21.4 and 0% inhibition of the EBV-EA activation by TPA respectively, at concentrations of 1000, 500, 100 and 10 mol ratio/ TPA.

2.3. Protein kinase inhibition

The study of protein tyrosine kinase inhibition by the synthesized compounds was performed in order to rationalize the chemopreventive action of the quinoxaline derivatives and explore their potential interactions with the receptor.

Enzyme inhibition study of compounds **1**, **3-10**, **13-16** and **18** against human tyrosine kinase was performed in two different human tumor cell lines HepG2 and MCF7 cell lines (c.f. Table 2). The results showed that most of the tested compounds exhibited inhibitory potencies against human TRK. Compounds **7**, **9**, **10** and **8** showed to possess more potent inhibition against human TRK in HepG2 and MCF7 cell lines than that of the untreated cells (Table 2) and of similar potency to the positive control, doxorubicin. Compounds **1**, **16** and **18** had no activity against TRK, while the other compounds had low affinity and moderate activity in both cell lines.

2.4. Molecular modeling: docking study

The molecular modeling study of the most potent compounds into the protein tyrosine kinase c-kit was performed in order to rationalize the chemopreventive action of the quinoxaline derivatives and explore their potential interactions with the receptor (c-kit) by generate plausible binding poses for the most active compounds (**7**, **8**, **9** and **10**). With the software LigandScout [38], a 3D interaction map was generated from the ligand (Gleevec) co-crystallized in the protein binding site (PDB code 1T46). The generated structure-based pharmacophore translated the important binding features for the inhibition of c-kit and was used to guide the selection of the more plausible binding poses of the newly synthesized compounds. The pharmacophore showed two main hydrophobic subsites accommodating the hydrophobic residues of the ligand in the binding pocket.

These residues were on one side VAL603, LEU799, PHE811 and THR670, and on the other side ILE653, LEU783, LEU647 and ILE808. In the center of the cavity, two hydrogen bonds were believed to stabilize the compound involving the residues GLU640 and ASP810. A complete exclusion volume coat drew boundaries that determine the capacity of the binding site.

The crystal structures of c-kit receptor protein (PDB code: 1T46) was prepared and used for the docking study. The docking program GOLD was used to find plausible docking poses for four compounds displaying the best inhibitory potencies: **7**, **8**, **9** and **10**. The generated docking conformations were prioritized based on their ability to fulfill the above mentioned 3D pharmacophore features. These results were highly correlated to the chemopreventive activity of the compound series.

Compounds **7** (Figure 3), which displayed the highest chemopreventive activity, was deeply embedded into the ATP-binding cleft of c-kit. The docking pose met the pharmacophore features and good complementarities were observed between the docked ligand and the hydrophobic subsites of the enzymatic cavity. In the first subsite, the dimethylamino group of **7** was stabilized by VAL603, LEU799, PHE811 and THR670, while the quinoxaline moiety interacted with the residues ILE653, LEU783, LEU647 and ILE 808 of the second enzyme hydrophobic subsite. The hydrogen bonds were identified between GLU640 and ASP810 and the hydrazone group of the ligand (Figure 3).

The docking conformation of compounds **8**, **9** and **10**, superposed to the one of compound **7** in Figure 4, showed the same hydrogen bond interactions. The substitution of the dimethylamino group, in *para* position of the phenyl ring (compounds **7** and **8**), to two dimethoxy groups in *ortho* position (compounds **9** and **10**) affected the activity. In order to decrease the steric hindrance, the dimethoxy groups enforced the aromatic ring to rotate and lost the π -stacking with PHE811, which destabilized compounds **9** and **10**. The effect of the polar carboxylate group on compounds **8** and **10** was believed to be unfavorable because of its orientation towards the hydrophobic binding cleft. This molecular modeling study into the active site of c-kit allowed to provide a rationale to the decreasing chemopreventive activity measured for **8**, **9** and **10** compared to **7**. Free NH on the quinoxaline moiety and the presence of the dimethyl group on the phenyl ring decreased the activity of compounds **4** and **5**, but was still close to the reference, which also

emphasized the role of the dimethyl group in hydrophobic interaction with the receptor. Building up a tricyclic system, except for compounds **11** and **12**, or spiro compounds, had a negative effect on the activity.

3. Conclusion

The cancer chemopreventive activity of the newly synthesized quinoxaline derivatives **1-20** was estimated by studying their inhibitory effects on Epstein–Barr virus early antigen (EBV-EA) activation induced by 12-*O*-tetradecanoylphorbol-13-acetate (TPA). The synthesized quinoxaline derivatives **1-20** showed dose dependent inhibitory activities, most of them showed promising activity at the highest concentration of 1000 mol ratio/TPA. Compounds **7** and **9** showed stronger effect than that of oleanolic acid, the reference inhibitor. Allyl or acetate substitution on the quinoxaline nitrogen, as well as the presence of N(CH₃)₂ at position 4 of the phenyl ring, showed a great effect on potency. The results of TRK inhibition showed that compounds **7, 8, 9** and **10** had potent activity in both HepG2 and MCF-7 cancer cell lines similar to doxorubicin. Then, a molecular docking study of the four best inhibitors revealed potential binding mode into the c-kit receptor, and explained the main structure activity relationships. Finally, compound **7** was discovered to be highly potent and will be subjected for further investigations as in vivo study.

4. Experimental

4.1. Physical measurements

Microanalyses, spectral data and X-ray structures of the compounds were performed in the Microanalytical and X-ray Laboratories, National research centre, Cairo, Egypt. The IR spectra (4000- 400 cm⁻¹) were recorded using KBr pellets in a Jasco FT/IR 300E Fourier transform infrared spectrophotometer on a Perkin Elmer FT-IR 1650 (spectrophotometer). The ¹H and ¹³C NMR spectra were recorded using Joel EX-270 MHz and 500 MHz NMR spectrophotometers. Chemical shifts are reported in parts per million (ppm) from the tetramethylsilane resonance in the indicated solvent. Coupling constants are reported in Hertz (Hz); spectral splitting partners are designed as follows: singlet (s); doublet (d); triplet (t); multiplet (m). The mass spectra were carried out using Finnigan mat SSQ 7000 (Thermo. Inst.Sys. Inc., USA) spectroscopy at 70 ev. Dimethyl sulfoxide

(DMSO), doxorubicin, penicillin, and streptomycin were obtained from Sigma Chemical Company (Saint Louis, MO, USA). Human Tyrosine kinase (TRK) ELISA kit was purchased from Glory Science Co., Ltd (Del Rio, TX 78840, USA).

4.1.1. Preparation of compounds 4-6

A mixture of compound **3** (50 mmole) in absolute ethanol (100 mL) and acetone, *N,N*-dimethylaminobenzaldehyde or 2,6-dimethoxybenzaldehyde, respectively (50 mmole) was refluxed for 7-9h. After reaction completion, the solvent was evaporated under vacuum and the solid residue obtained was washed with water, filtered off and recrystallized from ethanol.

4.1.1.1. 3-[2-(Propan-2-ylidene)hydrazinyl]quinoxalin-2(1H)-one (**4**) [32].

Reflux time 8 hr, $R_f = 0.15$ (petroleum ether / ethyl acetate, 1: 3), yield 78.7%, m.p. 256-258 °C (lit 256 °C) IR (cm^{-1}): 3451(NH quinoxaline), 3274(NH, hydrazinyl), 1674(C=O), 1617(C=N), 1570(C=N and C=C). ^1H NMR (270 MHz, $\text{DMSO}-d_6$): 1.99(t, 3H, CH_3), 2.09(t, 3H, CH_3), 6.95(m, 1H), 7.18(m, 2H), 7.42(m, 1H), 9.28(s, 1H, NH hydrazinyl, D_2O exchangeable), 12.41(s, 1H, NH quinoxaline, D_2O exchangeable). MS: m/z : 216(M^+ , 15%), 176(m^* , 100). Anal. Calcd for $\text{C}_{11}\text{H}_{12}\text{N}_4\text{O}$ (FW: 216.10): C, 61.10; H, 5.59; N, 25.91. Found: C, 61.15; H, 5.65; N, 25.85.

Reflux time 7

4.1.1.2. 3-(2-(4-(Dimethylamino)benzylidene)hydrazinyl)quinoxalin-2(1H)-one (**5**).

hr, $R_f = 0.25$ (petroleum ether / ethyl acetate, 1: 3), yield 71.1%, m.p. 250-253°C IR (cm^{-1}): 3423(NH quinoxaline), 3182 (NH hydrazide), 3056 (CH, aromatic), 2852 (CH, aliphatic), 1687(C=O), 1605(C=N), 1571(C=N, C=C). ^1H NMR (270 MHz, $\text{DMSO}-d_6$): 2.97(s, 6H, $\text{N}(\text{CH}_3)_2$), 6.77(d, 2H, $J = 7.6\text{Hz}$, 7.15(m, 2H); 7.6(m, 4H); 8.49 (s, 1H); 10.91(br., NH, D_2O exchangeable), 12.35(s., NH, D_2O exchangeable). ^{13}C NMR (270 MHz, $\text{DMSO}-d_6$): 40.5, 111.5, 115.2, 123.4, 128.4, 129.1, 131.6, 142.6, 147.4, 150.89, 153.4, 154.5 MS: m/z 307(M^+ , 5%), 176(m^* , 100). Anal. Calcd for $\text{C}_{17}\text{H}_{17}\text{N}_5\text{O}$ (FW: 307.14): C, 66.43; H, 5.58; N, 22.79. Found: C, 66.49; H, 5.61; N, 22.74.

4.1.1.3. 3-(2-(2,6-Dimethoxybenzylidene)hydrazinyl)quinoxalin-2(1H)-one (6**).** Reflux time 9 hr, $R_f = 0.7$ (petroleum ether/ ethyl acetate, 1: 3), yield, 67.9%, m.p. 220-222°C. IR (cm^{-1}): 3316(NH quinoxaline), 3205 (NH), 3046, 2999(CH, aromatic), 2894, 2832 (CH,

aliphatic), 1694(C=O), 1612(C=N), 1567(C=N, C=C). ^1H NMR (270 MHz, DMSO- d_6): 3.68(s, 3H, OCH₃), 3.71(s, 3H, OCH₃), 7.03-7.33(m, 5H); 7.49(m, 2H); 8.89 (s, 1H); 11.39(s., NH, D₂O exchangeable), 12.43(s., NH, D₂O exchangeable). ^{13}C NMR (270 MHz, DMSO- d_6): 56.4, 106.4, 110.0, 114.9, 122.6, 123.5, 125.8, 128.76, 131.13, 132.96, 133.7, 142.51, 146.2, 150.89, 157.6, 161.2 MS: m/z 324(M⁺, 17%), 176(m*, 100). Anal. Calcd for C₁₇H₁₆N₄O₃ (FW: 324.12): C, 62.95; H, 4.97; N, 17.27. Found: C, 62.89; H, 5.03; N, 17.25.

4.1.2. Preparation of compounds 7 -10. *General procedure:* A mixture of compound 5 or 6 (4 mmole), K₂CO₃ (4.2 mmole) and allyl bromide or ethyl chloroacetate (4.2 mmole) in 10 ml of DMF was stirred for 10-12h. The inorganic salt was filtered off and the solution was evaporated under reduced pressure. The precipitate obtained was washed with water and crystallized from acetone.

4.1.2.1. 1-Allyl-3-(2-(4-(dimethylamino)benzylidene)hydrazinyl)quinoxalin-2(1H)-one (7). Reflux time = **12 hr**, Rf = 0.85 (petroleum ether / ethyl acetate, 1: 3), yield, 69.7%, m.p. 219-221 °C. IR (cm⁻¹): 3255(NH, hydrazide), 3071(CH, aromatic), 3034(CH=CH₂), 2852(CH, aliphatic), 1646(C=O), 1607(C=N), 1569(C=N, C=C). ^1H NMR (500 MHz, DMSO- d_6): 3.27(s, 6H, N(CH₃)₂), 4.87(d, 2H, $J = 2\text{ Hz}$, CH₂), 5.06(dd, 1H), 5.16(dd, 1H), 5.92 (m, 1H), 6.72(d, 2H, $J = 5\text{ Hz}$), 7.19(d, 2H, $J = 5\text{ Hz}$), 7.55(m, 1H); 7.61(m, 3H); 8.39(s, 1H); 10.94(br., NH, D₂O exchangeable). ^{13}C NMR (270 MHz, DMSO- d_6): 40.5, 53.01, 111.8, 113.6, 118.2, 123.7, 124.7, 128.7, 129.4, 130.6, 131.2, 132.4, 142.8, 146.4, 150.7, 152.8, 153.6. MS: m/z: 334(M⁺, 8%), 176(m*, 100). Anal. Calcd for C₂₀H₂₁N₅O (FW: 347.17): C, 69.14; H, 6.09; N, 20.16. Found: C, 69.11; H, 6.14; N, 20.18.

4.1.2.2. Ethyl 2-(3-(2-(4-(dimethylamino)benzylidene)hydrazinyl)-2-oxoquinoxalin-1(2H)-yl)acetate (8). Reflux time = **10 hr**, Rf = 0.5 (petroleum ether / ethyl acetate, 1: 3), yield 81.3%, m.p. 210-213°C. IR (cm⁻¹): 3264(NH, hydrazide), 3036(CH, aromatic), 2811(CH, aliphatic), 1752(C=O), 1647(C=O), 1608(C=N), 1571(C=N and C=C). ^1H NMR (500 MHz, DMSO- d_6): 1.19(t, 3H, CH₃), 3.2(s, 6H, N(CH₃)₂), 3.84(s, 2H, CH₂), 4.16(q, 2H, CH₂), 7.02(m, 2H), 7.25(m, 2H), 7.33(m, 2H), 7.57(m, 1H), 7.91(m, 1H), 8.88(s, 1H), 11.36(s, 1H, NH, D₂O exchangeable). ^{13}C NMR (500 MHz, DMSO- d_6): 14.23, 40.44, 49.2, 62.5, 111.8, 113.8, 122.3, 125.5, 127.7, 128.4, 129.3, 126.1, 130.33, 132.63, 142.55,

146.4, 150.89, 153.2, 169.2. MS: m/z : 393(M^+ , 10%), 176(m^* , 100). Anal. Calcd for $C_{21}H_{23}N_5O_3$ (FW: 393.18): C, 64.11; H, 5.89; N, 17.80. Found: C, 64.17; H, 5.87; N, 17.74

4.1.2.3. 1-Allyl-3-(2-(2,6-dimethoxybenzylidene)hydrazinyl)quinoxalin-2(1H)-one (9).

Reflux time = **11 hr**, R_f = 0.25 (petroleum ether / ethyl acetate, 1: 3), yield 67%, m.p. 155-157°C. IR (cm^{-1}): 3264(NH), 3062(CH, aromatic), 2832(CH, aliphatic), 1649(C=O), 1606(C=N), 1569(C=N, C=C). 1H NMR (270 MHz, DMSO- d_6): 3.80(s, 3H, CH_3), 3.82(s, 3H, CH_3), 4.20(m, 2H, CH_2), 5.16(m, 2H, CH_2), 6.37(m, 1H, CH=), 7.04(m, 3H), 7.38(m, 3H), 7.60(m, 1H); 8.91(s, 1H); 11.43(s, 1H, NH, D_2O exchangeable). ^{13}C NMR (270 MHz, DMSO- d_6): 52.5, 55.9, 110.3, 107.8, 113.6, 125.4, 128.1, 129.7, 130.61, 132.7, 134.13, 142.51, 143.5, 150.12, 153.4, 159.8. MS: m/z : 364(M^+ , 40%), 176(m^* , 100). Anal. Calcd for $C_{20}H_{20}N_4O_3$ (FW: 364.15): C, 65.92; H, 5.53; N, 15.38. Found: C, 65.96; H, 5.50; N, 15.45.

4.1.2.4. Ethyl 2-(3-(2-(2,6-dimethoxybenzylidene)hydrazinyl)-2-oxoquinoxalin-1(2H)-yl)acetate (10).

Reflux time = **12 hr**, R_f = 0.6 (petroleum ether / ethyl acetate, 1: 3), yield 68.4%, m.p. 190-192°C. IR (cm^{-1}): 3280(NH, hydrazide), 3061 (CH, aromatic), 2826(CH, aliphatic), 1748(C=O), 1637(C=O), 1602(C=N), 1570(C=N, C=C). 1H NMR (270 MHz, DMSO- d_6): 1.43(t, 3H, CH_3), 3.79(s, 3H, CH_3), 3.82(s, 3H, CH_3), 4.93(s, 2H, CH_2), 5.18(q, 2H, CH_2), 7.07(m, 2H), 7.30(m, 2H), 7.60(m, 3H), 8.89(s, 1H), 11.43(s, 1H, NH hydrazide, D_2O exchangeable). ^{13}C NMR (270 MHz, DMSO- d_6): 14.7, 48.5, 60.8, 106.9, 110.9, 113.6, 124.9, 126.1, 128.6, 129.4, 131.21, 132.9, 142.55, 143.3, 146.9, 151.27, 153.1, 160.5, 167.22. MS: m/z : 350(M^+ , 14%), 176(m^* , 100). Anal. Calcd for $C_{21}H_{22}N_4O_5$ (FW: 410.16): C, 61.45; H, 5.40; N, 13.65. Found: C, 61.41; H, 5.42; N, 13.70.

4.1.3. Preparation of compounds 11-16

A mixture of compound **3** (5mmole) and ethyl bromoacetate, chloroacetyl chloride, ethyl oxamate, diethyl oxalate, ethyl chloroformate or triethyl orthoformate (5 mmol) was dissolved in DMF (30 mL). The reaction mixture was stirred at 90 °C for 8 h. After reaction completion, the formed solid was filtered off. The crude product obtained was

washed with methanol and purified by recrystallization from DMF/ methanol (1:2) mixture.

4.1.3. 1. 1-Hydroxy-3*H*-[1,2,4]triazino[4,3-*a*]quinoxalin-5(6*H*)-one (11) .

R_f = 0.3 (petroleum ether / ethyl acetate, 1: 3), yield 88.3%, m.p.184-186°C. IR (cm⁻¹): 3567(OH), 3438(NH quinoxaline), 3220(NH), 3032 (CH, aromatic), 1673(C=O), 1606 (C=N), 1580(C=C). ¹H NMR (500 MHz, DMSO-*d*₆): 7.09(m, 4H); 7.33(m, 1H), 12.06(br., NH(s), OH, D₂O exchangeable). ¹³C NMR (500 MHz, DMSO-*d*₆): 82.5, 110.3, 118.6, 122.8, 125.98, 126.5, 142.22, 151.5, 155.23, 163.7. MS: m/z: 216(M⁺, 40%). Anal. Calcd for C₁₀H₈N₄O₂ (FW: 216.06): C, 55.55; H, 3.73; N, 25.91. Found: C, 55.41; H, 3.81; N, 25.88.

4.1.3.2. 1*H*-[1,2,4]triazino[4,3-*a*]quinoxaline-2,5(3*H*,6*H*)-dione (12).

R_f= 0.36 (petroleum ether / ethyl acetate, 1: 3), yield 81%, m.p.197-199°C. IR (cm⁻¹): 3429(NH quinoxaline), 3284(NH), 3053(CH, aromatic), 1671(C=O), 1596(C=N), 1500(C=C). ¹H NMR (500 MHz, DMSO-*d*₆): 3.9(s, 2H, CH₂), 7.26(m, 3H), 7.62(m, 1H), 9.5(br., NH,D₂O exchangeable), 11.9(br., NH,D₂O exchangeable). ¹³C NMR (500 MHz, DMSO-*d*₆): 48.3, 116.9, 118.3, 121.3, 122.8, 125.5, 138.9, 152.1, 159.23, 161.0. MS: m/z: 216 (M⁺, 21%). Anal. Calcd for C₁₀H₈N₄O₂ (FW: 216.06): C, 55.55; H, 3.73; N, 25.91. Found: C, 55.39; H, 3.84; N, 25.85.

4.1.3. 3. 2-Hydroxy-1-imino-1*H*-[1,2,4]triazino[4,3-*a*]quinoxalin-5(6*H*)-one (13).

R_f = 0.27 (petroleum ether/ ethyl acetate, 1: 3), yield 79%, m.p.223-225°C. IR (cm⁻¹): 3443(OH), 3400(NH quinoxaline), 3298 (NH), 3053 (CH, aromatic), 1681(C=O), 1511(C=N), 1580(C=C). ¹H NMR (500 MHz, DMSO-*d*₆): 4.54(s, NH,D₂O exchangeable), 7.09(m, 3H); 7.33(m, 1H), 8.7 (s, OH,D₂O exchangeable), 10.9(br., NH,D₂O exchangeable). ¹³C NMR (500 MHz, DMSO-*d*₆): 109.1, 116.9, 118.3, 121.3, 125.2, 125.5, 138.9, 152.1, 159.23, 161.0. MS: m/z: 228(M⁺-1, 26%). Anal. Calcd for C₁₀H₇N₅O₂ (FW: 229.06): C, 52.40; H, 3.08; N, 30.56. Found: C, 52.38; H, 3.12; N, 30.44.

4.1.3. 4. 2-Hydroxy-1*H*-[1,2,4]triazino[4,3-*a*]quinoxaline-1,5(6*H*)-dione(14).

R_f = 0.31 (petroleum ether / ethyl acetate, 1: 3), yield 73%, m.p.234-237°C IR (cm⁻¹):

3440(OH), 3400(NH quinoxaline), 3018(CH, aromatic), 1671(C=O), 1611(C=N), 1581(C=C). ^1H NMR (270 MHz, DMSO- d_6): 7.28(m, 3H), 7.36(m, 1H), 8.7(br., OH, D_2O exchangeable), 12.18(br., NH, D_2O exchangeable). ^{13}C NMR (500 MHz, DMSO- d_6): 116.9, 121.3, 122.8, 125.5, 129.5, 133.9, 152.7, 153.4, 155.1, 157.5. MS: m/z : 230(M^+ , 26%). Anal. Calcd for $\text{C}_{10}\text{H}_6\text{N}_4\text{O}_3$ (FW: 230.04): C, 52.18; H, 2.63; N, 24.34. Found: C, 52.16; H, 2.55; N, 24.39.

4.1.3. 5. [1,2,4]triazolo[4,3-*a*]quinoxaline-1,4(2*H*,5*H*)-dione (15).

R_f = 0.32 (petroleum ether/ ethyl acetate, 1: 3), yield 69%, m.p.247-249°C. IR (cm^{-1}): 3423 (NH), 3200 (NH), 3041 (CH, aromatic), 1682(C=O), 1650(C=O), 1608(C=N), 1581(C=C). ^1H NMR (270 MHz, DMSO- d_6): 7.12(m, 3H); 7.3(m, 1H), 12.0(br., NH(s), D_2O exchangeable). ^{13}C NMR (270 MHz, DMSO- d_6): 114.1, 124.9, 129.5, 132.1, 145.8, 151.3, 154.5. MS: m/z : 202(M^+ , 26%). Anal. Calcd for $\text{C}_9\text{H}_6\text{N}_4\text{O}_2$ (FW: 202.05): C, 53.47; H, 2.99; N, 27.71. Found: C, 53.39; H, 2.84; N, 27.55.

4.1.3.6. [1,2,4]triazolo[4,3-*a*]quinoxalin-4(5*H*)-one (16).

R_f = 0.17 (petroleum ether / ethyl acetate, 1: 3), yield 78%, m.p.241-243°C. IR (cm^{-1}): 3402(NH), 3055(CH, aromatic), 1681 (C=O), 1615(C=N), 1524(C=C). ^1H NMR (270 MHz, DMSO- d_6): 7.2(m, 1H), 7.3(m, 3H); 8.1(m, 1H), 12.0(br., NH, D_2O exchangeable). ^{13}C NMR (270 MHz, DMSO- d_6): 125.6, 128.2, 129.4, 132.3, 137.4, 144.5, 148.3, 157.4, 163.4. MS: m/z : 186(M^+ , 100%). Anal. Calcd for $\text{C}_9\text{H}_6\text{N}_4\text{O}$ (FW: 186.05): C, 58.06; H, 3.25; N, 30.09. Found: C, 58.10; H, 3.33; N, 30.05.

4.1.4. Preparation of compounds 17 and 18

A solution of methyl isothiocyanate or benzoyl isothiocyanate (5 mmol) in toluene (15mL) was added to a solution of compound **3** (5 mmol) in toluene (15 mL). The reaction mixture was refluxed for 12 h. The solvent was evaporated under reduced pressure. The solid was washed with cold water and recrystallized from ethanol.

4.1.4.1. 4'-methyl-5'-thioxo-1*H*-spiro[quinoxaline-2,3'-[1,2,4]triazolidin]-3(4*H*)-one(17).

R_f = 0.42 (petroleum ether/ ethyl acetate, 1: 3), yield 58%, m.p.173-175°C. IR (cm^{-1}):

3400-3219(NH(s)), 2923 (CH, aromatic), 2875(CH, aliph.)1680 (C=O), 1647(C=N, thiadiazole moiety), 1609(C=N), 1536(C=C). ¹H NMR (270 MHz, DMSO-*d*₆): 2.78(s, 3H, CH₃), 3.9(s, 1H, NH, D₂O exchangeable), 6.99(m, 1H), 7.28(m, 1H), 7.56(br., NH,D₂O exchangeable), 7.6(m, 1H), 8.0(m, 1H), 9.5(br., NH,D₂O exchangeable). ¹³C NMR (270 MHz, DMSO-*d*₆): 25.9, 83.8, 114.9, 118.2, 121.2, 125.9, 137.4, 145.1, 155.6, 167.2. MS: m/z: 249 (M⁺, 20%). Anal. Calcd for C₁₀H₁₁N₅OS (FW: 249.07): C, 48.18; H, 4.45; N, 28.09; S, 12.86. Found: C, 48.22; H, 4.31; N, 28.22; S, 12.92.

4.1.4.2. 4'-Benzoyl-5'-thioxo-1*H*-spiro[quinoxaline-2,3'-[1,2,4]triazolidin]-3(4*H*)-one (18).

R_f = 0.38 (petroleum ether/ ethyl acetate, 1: 3), yield 55%, m.p.213-215°C. IR (cm⁻¹): 3432 (NH, quinoxaline), 3220(NH), 2950 (CH, aromatic), 2820(CH, aliph.), 1683(C=O), 1669(C=O), 1642(C=N, thiadiazole moiety), 1605(C=N), 1576(C=C). ¹H NMR (270 MHz, DMSO-*d*₆): 7.05(m, 1H), 7.11(m, 1H), 7.24(m, 1H), 7.35(m, 1H), 7.5(m, 2H), 7.7(br., NH,D₂O exchangeable), 8.06(m, 3H), 11.05(br., NH,D₂O exchangeable), 12.7(br., NH,D₂O exchangeable). ¹³C NMR (270 MHz, DMSO-*d*₆): 84.9, 114.1, 117.3, 121.1, 129.7, 132.1, 133.4, 134.6, 145.5, 151.8, 158.4, 165.2. MS: m/z: 339.08 (M⁺, 15%). Anal. Calcd for C₁₆H₁₃N₅O₂S (FW: 339.08): C, 56.63; H, 3.86; N, 20.64; S, 9.45. Found: C, 56.58; H, 3.84; N, 20.59; S, 9.46.

4.1.5. Preparation of compounds 19 and 20

A mixture of compound **3** (5 mmol) and diethyl malonate or diethyl succinate (5 mmol) was dissolved in DMF (30 mL) and few drops of triethyl amine. The reaction mixture was stirred at 90 °C for 12 hr. After reaction completion, the formed solid was filtered off. The crude product obtained was washed with methanol and finally purified by recrystallization from DMF / methanol (1:2) mixture.

4.1.5.1. 1-(3-oxo-3,4-dihydroquinoxalin-2-yl)pyrazolidine-3,5-dione (19).

R_f = 0.39, Yield: 75%, m.p. 266-268. IR (cm⁻¹): 3400 (NH, quinoxaline), 3299(NH), 3016 (CH, aromatic), 2898(CH,pyrazolidine), 1680 (C=O), 1615(C=N), 1576(C=C). ¹H NMR (270 MHz, DMSO-*d*₆): 4.15(s, 2H, CH₂), 4.54(br., NH, D₂O exchangeable), 7.12(m, 3H), 7.36(m, 1H), 8.78(br., NH,D₂O exchangeable). ¹³C NMR (270 MHz, DMSO-*d*₆): 47.9,

116.1, 123.2, 125.7, 129.2, 132.4, 142.8, 155.2, 159.4, 169.4. MS: m/z : 244(M^+ , 20%). Anal. Calcd for $C_{11}H_8N_4O_3$ (FW: 244.06): C, 54.10; H, 3.30; N, 22.94. Found: C, 54.12; H, 3.35; N, 22.86.

4.1.5. 2. 1-(3-Oxo-3,4-dihydro-quinoxalin-2-yl)-tetrahydro-pyridazine-3,6-dione (20).

R_f = 0.41, Yield: 78%, m.p. 254-256°C. IR (cm^{-1}): 3400 (NH, quinoxaline), 3298(NH), 3015 (CH, aromatic), 2898(CH, pyrazolidine), 1680 (C=O), 1615(C=N), 1576(C=C). 1H NMR (270 MHz, DMSO- d_6): 4.15(s, 2H, CH₂), 4.54(s, 1H, NH, D₂O exchangeable), 7.12(m, 3H), 7.36(m, 1H), 8.78(br., NH, D₂O exchangeable). ^{13}C NMR (270 MHz, DMSO- d_6): 25.8, 30.1, 115.6, 124.6, 126.3, 129.2, 132.4, 142.4, 154.8, 158.9, 165.2. MS: m/z : 258 (M^+ , 20%). Anal. Calcd for $C_{12}H_{10}N_4O_3$ (FW: 258.08): C, 55.81; H, 3.90; N, 21.70. Found: C, 55.77; H, 3.82; N, 21.77.

4.2.1 Cells

EBV genome-carrying lymphoblastoid cells (Raji cells derived Burkitt's lymphoma) were cultured in 10% fetal bovine serum (FBS) in RPMI-1640 under the conditions described previously [34]. Spontaneous activation of EBV-EA in our subline of Raji cells was less than 0.1%.

4.2.2. Inhibition of EBV-EA activation assay.

Inhibition of EBV-EA activation was assayed using Raji cells (Virus non producer type), an EBV genome-carrying human lymphoblastoid cell, which were cultivated in 10% fetal bovine serum. (FBS) RPMI 1640 medium. The indicator cells (Raji, $1 \times 10^6/mL$) were incubated at 37 °C for 48 h in 1 mL of medium containing n-butyric acid (4 mM as trigger), TPA (32 pM = 20 ng in 2 μ L of DMSO as inducer), and various amounts of the test compounds dissolved in 5 μ L of DMSO (ca. 0.7% DMSO). Smears were made from the cell suspension. The EBV-EA inducing cells were stained with high titer EBV-EA positive serum from NPC patients and detected by an indirect immunofluorescence technique. In each assay, at least 500 cells were counted, and the number of stained cells (positive cells) was recorded. Triplicate assays were performed for each data point. as a relative ratio to the positive control experiment (100%), which was carried out within-butyric acid (4 mM) plus TPA (32 pM). In the experiments, the EBV-EA induction was

normally around 35%, and this value was taken as the positive control (100%). n-Butyric acid (4 mM) alone induced 0.1% EA-positive cells. The viability of treated Raji cells was assayed by the trypan blue staining method. The cell viability of the TPA positive control was greater than 80%. Therefore, only the compounds that induced less than 80% (% of control) of the EBV-activated cells (those with a cell viability of more than 60%) were considered able to inhibit the activation caused by promoter substances. Student's t-test was used for all statistical analyses [34- 36].

4.3. Protein kinase inhibition

4.3.1. Cell lines and culturing

The effect of tested compounds on the inhibition of human tyrosine kinase (TRK) was determined utilizing two different human tumor cell lines including liver cancer HepG2 and breast cancer MCF-7 cell lines obtained from the American Type Culture Collection (Rockville, MD, USA). The tumor cells were maintained in Dulbecco's modified Eagle's medium (DMEM) supplemented with 10% heat inactivated fetal calf serum (GIBCO), penicillin (100 U/ml) and streptomycin (100 µg/ml) at 37 °C in humidified atmosphere containing 5% CO₂. Cells at a concentration of 0.50×10^6 were grown in a 25 cm² flask in 5 ml of complete culture medium.

The cells in culture medium were treated with 20 µl of deferent concentration (2.5, 5, 10, 20 and 40 µg/ml) of the tested compounds or the standard reference drug, doxorubicin dissolved in DMSO, then incubated for 48 h at 37 °C, in a humidified 5% CO₂ atmosphere. The cells were harvested and homogenates were prepared in saline using a tight pestle homogenizer until complete cell disruption.

To determine the level of TRK, A double-antibody sandwich enzyme-linked immunosorbent assay (ELISA) was used. This assay is based on, add TRK to monoclonal antibody enzyme well which is pre-coated with human TRK monoclonal antibody, incubation; then, add TRK antibodies labeled with biotin, and combined with Streptavidin-HRP to form immune complex; then carry out incubation and washing again to remove the uncombined enzyme. Then add Chromogen solution A, B, the color of the liquid changes into the blue, and at the effect of acid, the color finally becomes yellow. The chroma of

color and the concentration of the human TRK of sample were positively correlated and the optical density was determined at 450 nm. The level of Human Tyrosine kinase (TRK) in samples was calculated as triplicate determinations from the standard curve and the IC₅₀ of TRK for each compound was calculated as the 50% inhibition in the level of TRK as compared with control untreated cancer cells.

4.4. Molecular docking study

4.4.1. Docking study

The studied ligands were protonated using Protonate 3D [41] and minimized in MOE (Chemical Computing Group, Montreal, CA) until the root-mean-square gradient of 0.000001 was reached using a MMFF94x force field. The crystal structures of c-kit receptor protein-tyrosine kinase in complex with STI-571 (Imatinib or Gleevec) was obtained from the Protein Data Bank (PDB code: 1T46). Hydrogen atoms were added in GOLD, V 5.1 (CCDC, Cambridge, UK) and default parameters were used unless otherwise stated. Before the docking study, the co-crystallized substrate STI-571 was removed from the structure. No structural water molecules were observed in the active site, and hence all water molecules were deleted. The docking program GOLD, V 5.1 (CCDC, Cambridge, UK) was used to perform the docking of compounds 7, 8, 9 and 10 into the crystal structure of c-kit. Based on the position of the co-crystallized ligand, the active site was defined choosing all residues around the original ligand in a circle of 7 Å. All docking runs were performed three times using standard default variables and GoldScore. The docking protocol utilized the study of 10 best docking poses per ligand. The top ten docked solutions for each ligand were retained for analysis. Software LigandScout [38] was used to generate a 3D pharmacophore from the PDB structure 1T46 using default options. This pharmacophore was used to rank the best docking poses of the studied compounds. Docking poses visualization was done by LigandScout. For each ligand, the most plausible conformation was selected based on its ability to fulfill highest amount of chemical features described in the 3D pharmacophore.

References

- [1] T. M. Kolb, Myrtle A. Davis, *Toxicol. Sci.* 81(2004) 233–242.
- [2] S. D. Undevia, F. Innocenti, J. Ramirez, L. House, A. A. Desai, L. A. Skoog, D. A.

- Singh, T. Karrison, H. L. Kindler, M. J. Ratain, *Eur. J. Cancer* 44 (2008) 1684-1692 .
- [3] S. Khier, C. Deleuze-Masquéfa, G. Moarbess, F. Gattacceca, D. Margout, I. Solassol, J-F. Cooperd, F. Pinguet, P-A. Bonnet, F. M. M. Bressolle, *Eur. J. Pharm.Sci* 39 (2010) 23–29.
- [4] G. Marverti, A. Ligabue, G. Paglietti, P. Corona, S. Piras, G. Vitale, D. Guerrieri, R. Luciani, M. P. Costi, C. Frassinetti, M. S. Moruzzi, *Eur. J. Pharmacol.* 615 (2009) 17–26.
- [5] H. I. Ali, N. Ashida, T. Nagamatsu, *Bioorg. Med. Chem.* 16 (2008) 922–940.
- [6] C. Deleuze-Masquefa, G. Moarbess, S. Khier, N. David, S. Gayraud-Paniagua, F. Bressolle, F. Pinguet, P-A. Bonnet, *Eur. J. Med. Chem.* 44 (2009) 3406–3411.
- [7] J. Guillon, M. Le Borgne, C. Rimbault, S. Moreau, S. Savrimoutou, N. Pinaud, S. Baratin, M. Marchivie, S. Roche, A. Bollacke, A. Pecci, L. Alvarez, V. Desplat, J. Jose, *Eur. J. Med. Chem.* 65 (2015) 205-222.
- [8] T. R. Mielcke, A. Mascarello, E. Filippi-Chiela, R. F. Zanin, G. Lenz, P. C. Leal, L. D. Chirardia, R. A. Yunes, R. J. Nunes, A. M. O. Battastini, F. B. Morrone, M. M. Campos *Eur. J. Med. Chem* 48(2012) 255-264
- [9] M. N. Noolvi, H. M. Patel, V. Bhardwaj, A. Chauhan *Eur. J. Med. Chem* 46 (2011) 2327-2346
- [10] M. O. Shibinskaya, A. S. Karpenko, S. A. Lyakhov, S. A. Andronati, N. M. Zholobak, N. Ya. Spivak, N. A. Samochina, L. M. Shafran, M. Ju. Zubritsky, V. F. Galat *Eur. J. Med. Chem* 46(2011) 794-798
- [11] R. Capdeville, E. Buchdunger, J. Zimmermann, A. Matter, *Drug Discov.* 1 (2002) 493–502.
- [12] A. Levitzki, *Acc. Chem. Res.* 36 (2003) 462-469.
- [13] M. Sattler, R. Salgia, *Leukemia Res.* 28S1 (2004) S11–S20
- [14] M. Bettencourt- Dias, R. Giet, R. Sinka, A. Mazumder, W. G. Look, F. Balloux, P. J. Zafiropoulos, S. Yamaguchi, S. Winter, R. W. Carthew, M. Cooper, D. Jones, L. Frenz, D. M. Glover, *Nature* 432 (2004) 980–987.
- [15] J. Baselga, J. Arribas, *Nat. Med.* 10(2004) 786–787.
- [16] P. Cohen, *Nat. Rev. Drug Discov.* 1(2002) 309–315.

- [17] D.C. Lev, L.S. Kim, V. Melnikova, M. Ruiz, H.N. Ananthaswamy, J.E. Price, Br. J. Cancer 91(2004) 795–802.
- [18] I. Posner, A. Levitzki, FEBS Lett. 353(1994) 155-161.
- [19] S. A. Galal, A. S. Abdelsamie, H. Tokuda, N. Suzuki, A. Lida, R. A. Ramadan, M. H. E. Atta, H. I. El Diwani, Eur. J. Med. Chem. 46 (2011) 327-340.
- [20] T. M. Kolb, M. A. Davis, Toxicol. Sci. 81(2004) 233-242.
- [21] C. A. Obafemi, W. Pfleiderer, Helv. Chim. Acta 77 (1994) 1549 -1556.
- [22] S. Mackay, C. J. Gilmore, C. Edwards, N. Stewart, K. Shankland, "maXus Computer Program for the Solution and Refinement of Crystal Structures, Bruker Nonius, The Netherlands, MacScience, Japan & The University of Glasgow, (1999).
- [23] C. K. Johnson, ORTEP-II. A Fortran Thermal-Ellipsoid Plot Program. Report ORNL-5138, Oak Ridge National Laboratory, Oak Ridge, Tennessee, USA, 1976
- [24] D. Waasmaier, A. Kirfel, Acta Cryst. A 51(1995) 416-431.
- [25] A. Altomare, G. Cascarano, C. Giacovazzo, A. Guagliardi, M. C. Burla, G. Polidori, M. Camalli, J. Appl. Cryst. 27(1994) 435-436.
- [26] G. W. H. Cheeseman, M. Rafiq, J. Chem. Soc., Sect. C3 (1971) 452-454.
- [27] O. O. Ajani, C. A. Obafemi, O. C. Nwinyi, D. A. Akinpelu, Bioorg. Med. Chem. 18 (2010) 214–221
- [28] É. Csikós, C. Gönczi, B. Podányi, G. Tóth, I. Hermecz, J. Chem. Soc. Perkin Trans. 1(1999) 1789-1793.
- [29] S.A. Galal, K.H. Hegab, A. S. Kassab, M. L. Rodriguez, S.M. Kerwin, A-M. A. El-Khamry, H. I. El Diwani, Eur. J. Med. Chem. 44 (2009) 1500–1508.
- [30] A. McKillop, S. K. Chattopadhyay, A. Henderson, C. Avendano, Synthesis 1997, 301-304.
- [31] A. McKillop, A. Henderson, P. S. Ray, C. Avendano, E. G. Molinero, Tetrahedron Lett. 23(1982) 3357-3360.
- [32] Q. P. Peterson, D.C. Hsu, D. R. Goode, C. J. Novotny, R. K. Totten, P. J. Hergenrother, J. Med. Chem. 52 (2009) 5721–5731
- [33] V. A. Mamedov, A.M. Murtazina, A.T. Gubaidullin, E. A. Hafizova, I. Kh. Rizvanov, Tetrahedron Lett. 50 (2009) 5186–5189.
- [34] Y. Ito, M. Kawanishi, T. Harayama, S. Takabayashi, Cancer Lett. 12 (1981) 175–180.

- [35] M. Takasaki, T. Konoshima, S. Kuroki, H. Tokuda, H. Nishino, *Cancer Lett.* 173(2001) 133-138.
- [36] N. Sakurai, M. Kozuka, H. Tokuda, T. Mukainaka, F. Enjo, H. Nishino, M. Nagai, Y. Sakurai, K. H. Lee, *Bioorg. Med. Chem.* 13 (2005) 1403-1408.
- [37] M. Takasaki, T. Konoshima, Y. Murata, M. Sugiura, H. Nishino, H. Tokuda, K. Matsumoto, R. Kasai, K. Yamasaki, *Cancer Lett.* 198 (2003) 37-42.
- [38] I. Shchemelinin, L. Šefc, E. Nečas, *Folia Biol. (Praha)* 52 (2006a) 81-101.
- [39] M. A. Bogoyevitch, R. K. Barr, A. J. Ketterman, *Biochim. Biophys. Acta* 1754 (2005) 79-99
- [40] G. Wolber, T. Langer, *J Chem Inf Model* 45 (2005) 160-169.
- [41] M.J. Bower, F.E. Cohen, R.L. Dunbrack, Jr., *J Mol Biol* 267 (1997) 1268-1282.

Figure Captions

Figure 1: Compound I

Figure 2: X-ray structure of compound 2

Figure 3: Plausible binding mode for compound 7 in 2D (up) and 3D (down) showing favorable hydrophobic interactions (yellow spheres) and two hydrogen bonds to GLU 640 (green) and ASP 810 (red). For interpretation of the references to color in this figure legend, the reader is referred to the web version of this article.

Figure 4: Plausible binding modes for compounds 7, 8, 9 and 10 superposed in the binding site of c-kit. Yellow spheres indicate hydrophobic features, red and green arrows hydrogen bond acceptor and donor respectively. For interpretation of the references to color in this figure legend, the reader is referred to the web version of this article.

Scheme 1: Synthesis of compounds 1-3

Scheme 2: Synthesis of compounds **4-10**

Scheme 3: Synthesis of compounds **11-16**

Scheme 4: Synthesis of compounds **17** and **18**

Scheme 5: Synthesis of compounds **19** and **20**

Table 1: Relative ratio^a of EBV-EA activation with respect to positive control (100%) in presence of compounds **1-21** and **Oleanolic acid**

Table 2. IC₅₀ values of human TRK of the tested compounds in human liver cancer HepG2 and breast cancer MCF-7 cell lines.

Table 1: Relative ratio^a of EBV-EA activation with respect to positive control (100%) in presence of compounds **1-21** and **Oleanolic acid**

Compounds #	% to control (% viability) 1000 mol ratio/TPA ^{bc}	500 mol ratio/TPA ^b	100 mol ratio/TPA ^b	10 mol ratio/TPA ^b
1	14.2(60)	46.8	78.5	100
2	16.7(50)	48.5	80.2	100
3	14.9(60)	46.5	78.1	100
4	13.2(60)	45.0	77.0	100
5	13.9(60)	42.2	71.7	100
6	16.8(60)	46.6	81.0	100
7	10.1(60)	41.6	73.2	100
8	12.7(60)	47.6	78.6	100
9	10.8(60)	42.0	73.5	100
10	13.5(60)	45.7	75.6	100
11	13.2(60)	46.0	77.6	100
12	13.6(60)	46.3	78.0	100
13	15.0(60)	47.1	79.0	100
14	14.2(60)	47.0	78.6	100
15	15.6(60)	47.2	79.1	100
16	18.6(60)	48.2	84.2	100
17	18.7(60)	48.3	84.6	100
18	19.1(60)	49.1	85.2	100
19	17.5(60)	48.0	83.9	100
20	16.7(60)	47.7	82.8	100
Oleanolic acid	12.7 (70)	30.0	80.0	100

a: Values represent percentages relative to the positive control value (100%).**b:** TPA concentration was 20 ng/mL (32 pmol/mL).**c:** Values in parentheses are the viability percentages of Raji cells

Table 2. IC₅₀ values of human TRK of the tested compounds in human liver cancer HepG2 and breast cancer MCF-7 cell lines.

Compound #	IC ₅₀ of TRK (pmol/ml) *	
	HepG2	MCF-7
1	NA	NA
3	9.00±0.07	10.20±1.10
4	15.00±1.38	17.20±1.60
5	9.80±0.08	11.80±1.20
6	7.50±0.06	8.75±0.07
7	2.65±0.03	2.90±0.04
8	4.50±0.04	4.85±0.05
9	3.50±0.03	4.15±0.04
10	4.10±0.04	4.60±0.05
13	18.00±1.60	20.20±2.00
14	20.00±2.00	27.80±2.85
15	25.00±1.40	30.00±2.50
16	NA	NA
18	NA	NA
Doxorubicin	2.50±0.01	3.20±0.02
Data were expressed as mean ± S.E. of triplicate independent experiments.		
*Indicate the concentration of the tested compounds required to inhibit human TRK by 50%. NA stands for no activity		

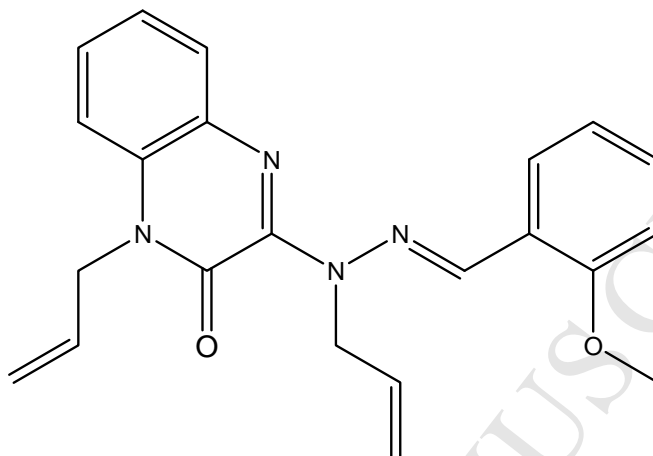


Figure 1: Compound I

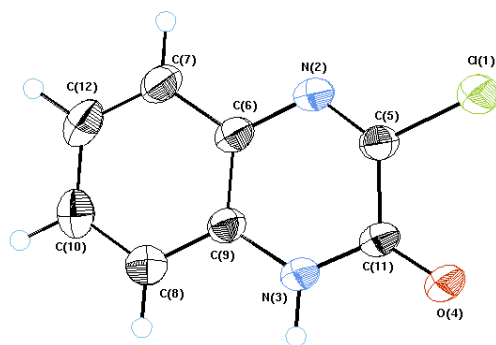


Figure 2: X-ray structure of compound 2

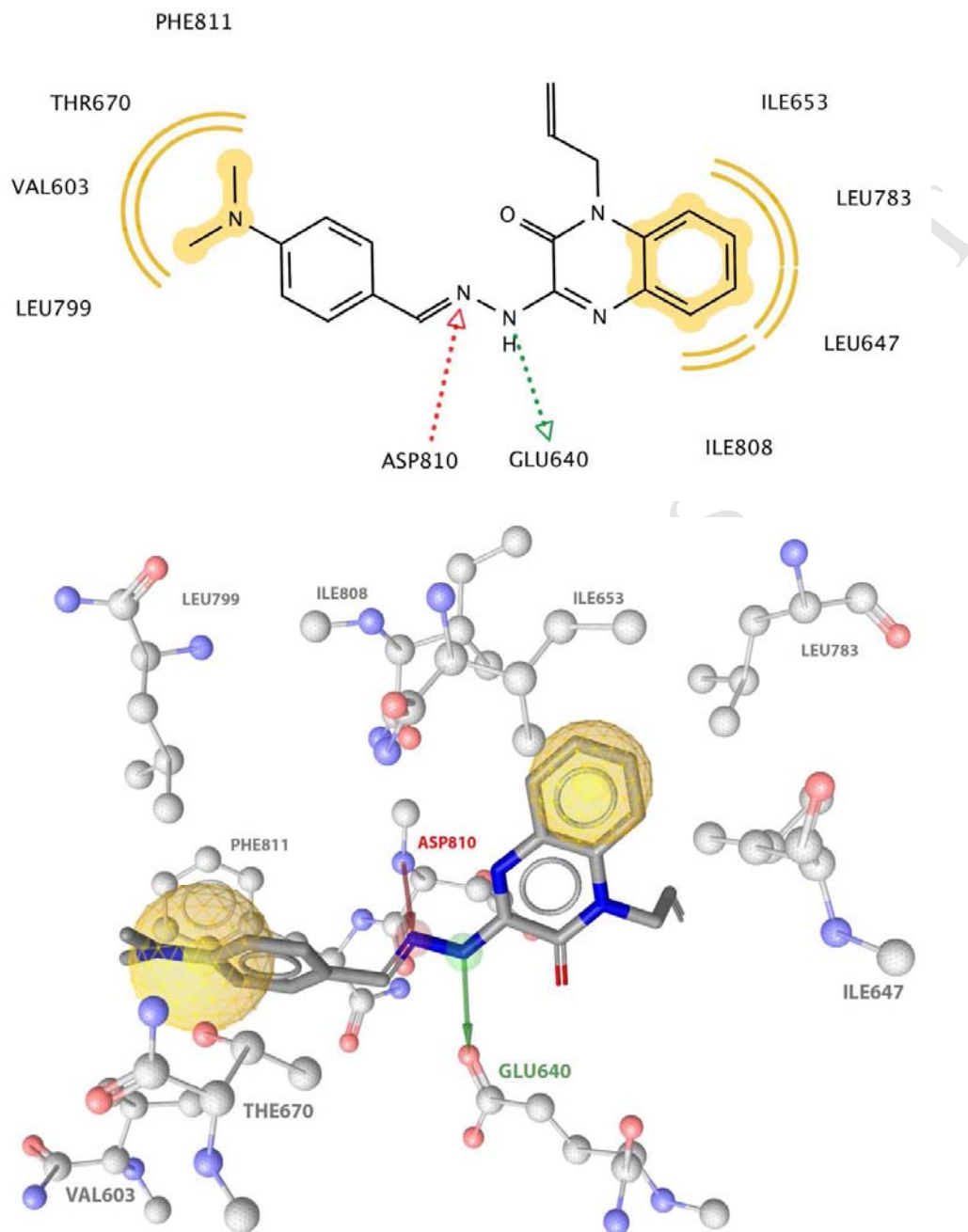


Figure 3: Plausible binding mode for compound **7** in 2D (up) and 3D (down) showing favorable hydrophobic interactions (yellow spheres) and two hydrogen bonds to GLU 640 (green) and ASP 810 (red). For interpretation of the references to color in this figure legend, the reader is referred to the web version of this article.

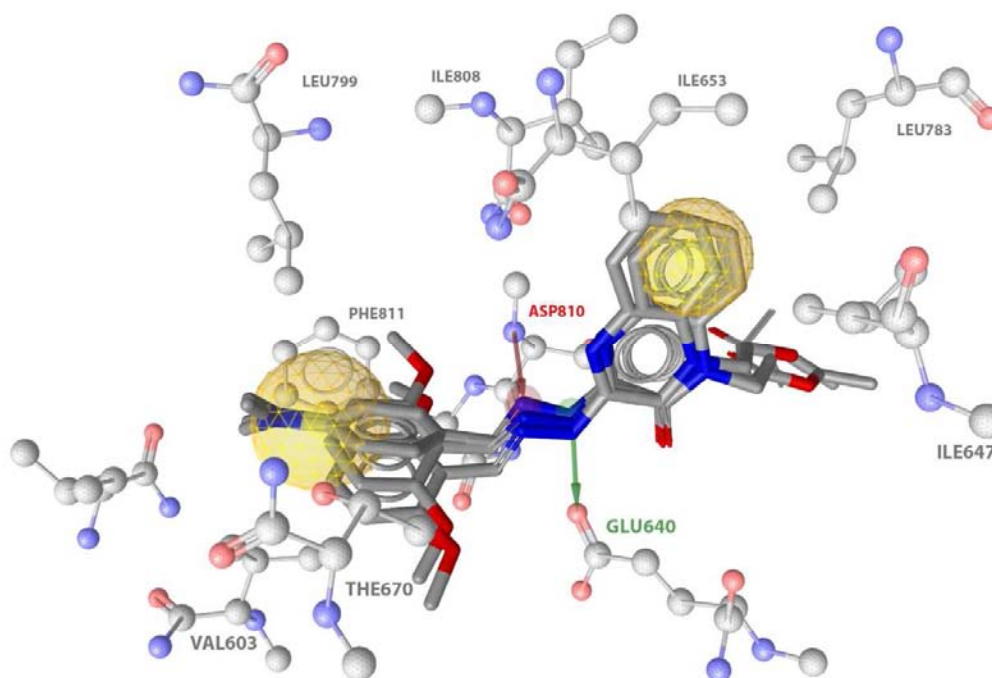
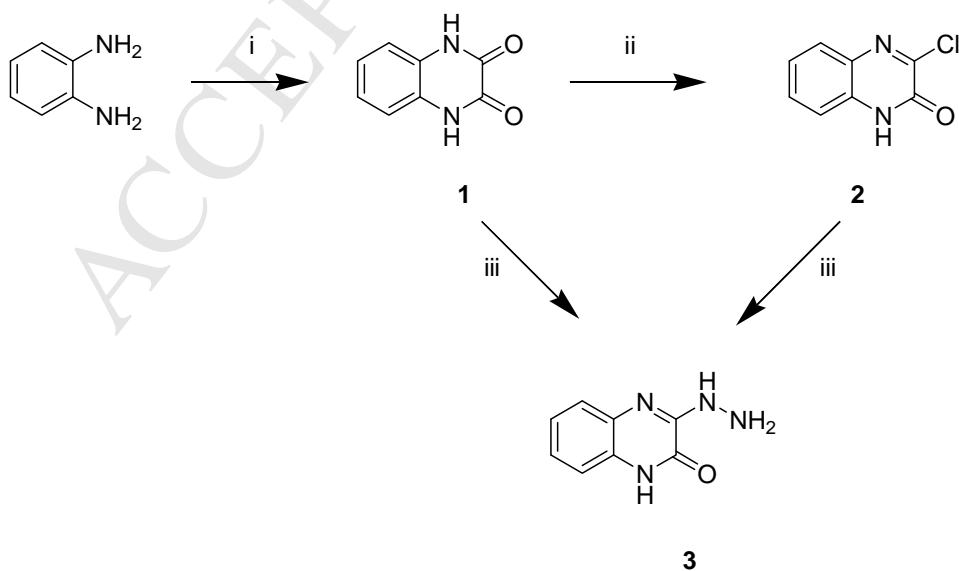
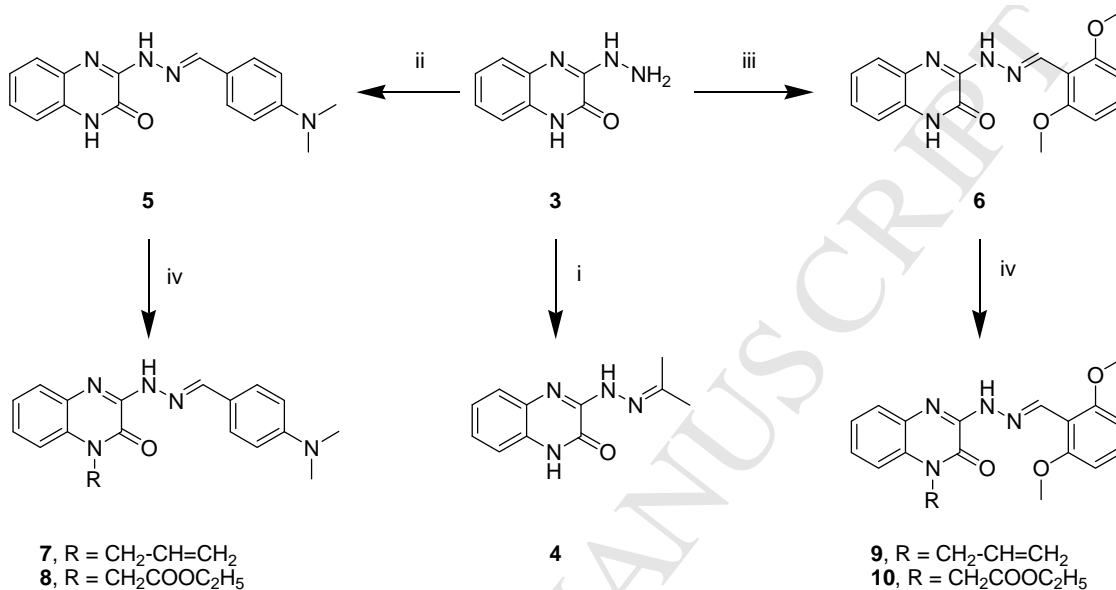


Figure 4: Plausible binding modes for compounds **7**, **8**, **9** and **10** superposed in the binding site of c-kit. Yellow spheres indicate hydrophobic features, red and green arrows hydrogen bond acceptor and donor respectively. For interpretation of the references to color in this figure legend, the reader is referred to the web version of this article.



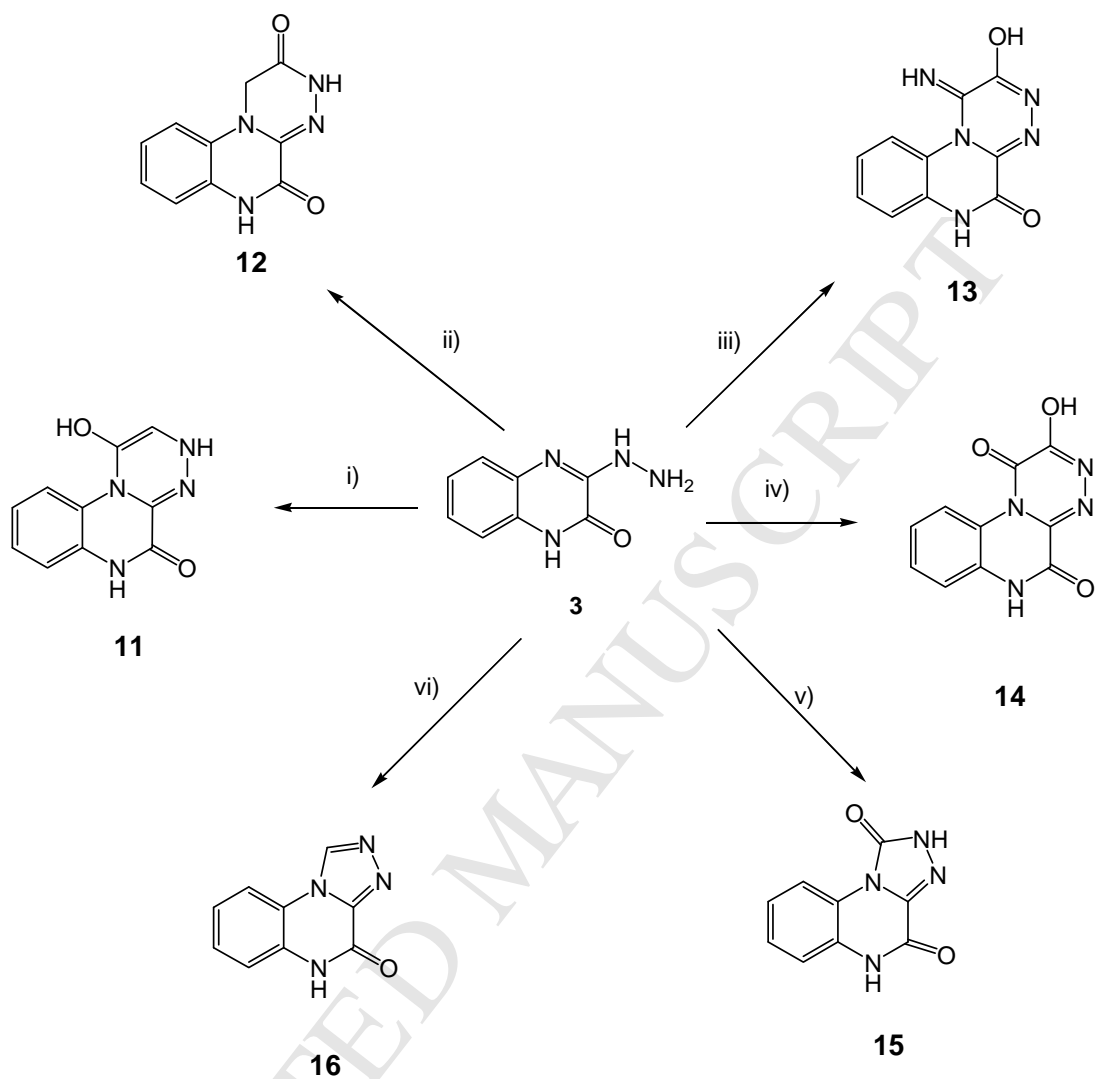
Reagents and conditions:

(i) oxalic acid, 4N HCl, reflux. (ii) POCl₃, methylene chloride, stirring, 4h, room temp. (iii) Hydrazine hydrate 98%, ethanol, stirring.

Scheme 1: Synthesis of compounds 1-3**Reagent and conditions:**

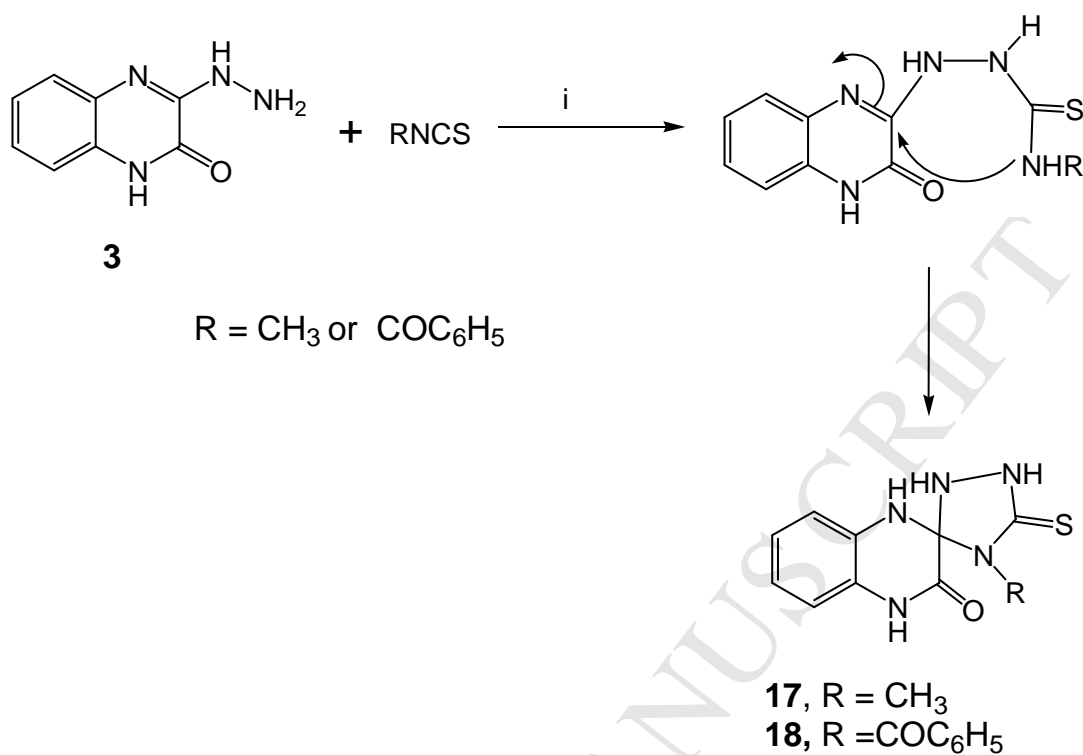
i) Acetone, ethanol, reflux. ii) *N,N*-dimethylbenzaldehyde, ethanol.
iii) 2,6-dimethoxybenzaldehyde, ethanol, reflux. iv) Allyl bromide or, ethyl chloroacetate,
K₂CO₃ anhydrous, DMF, stirring.

Scheme 2: Synthesis of compounds 4-10



Reagents and conditions: i) Ethyl bromoacetate, DMF, reflux. ii) chloroacetyl chloride DMF, reflux. iii) ethyl oxamate DMF, reflux. iv) diethyl oxalate DMF, reflux. v) ethyl chloroformate DMF, reflux. vi) triethyl orthoformate DMF, reflux.

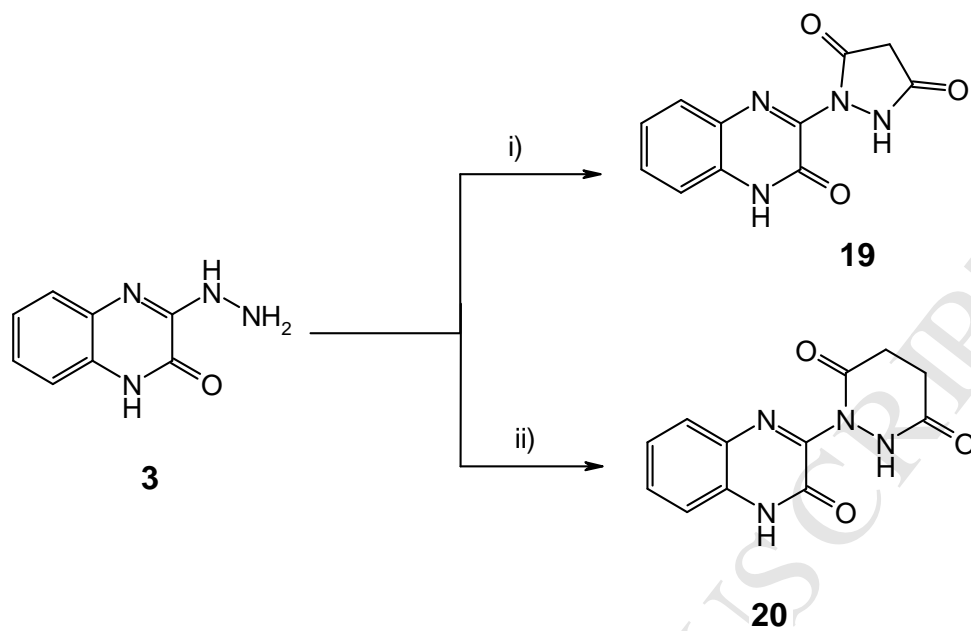
Scheme 3: Synthesis of compounds **11-16**



Reagents and conditions:

i) toluene reflux, 12h.

Scheme 4: Synthesis of compounds **17** and **18**



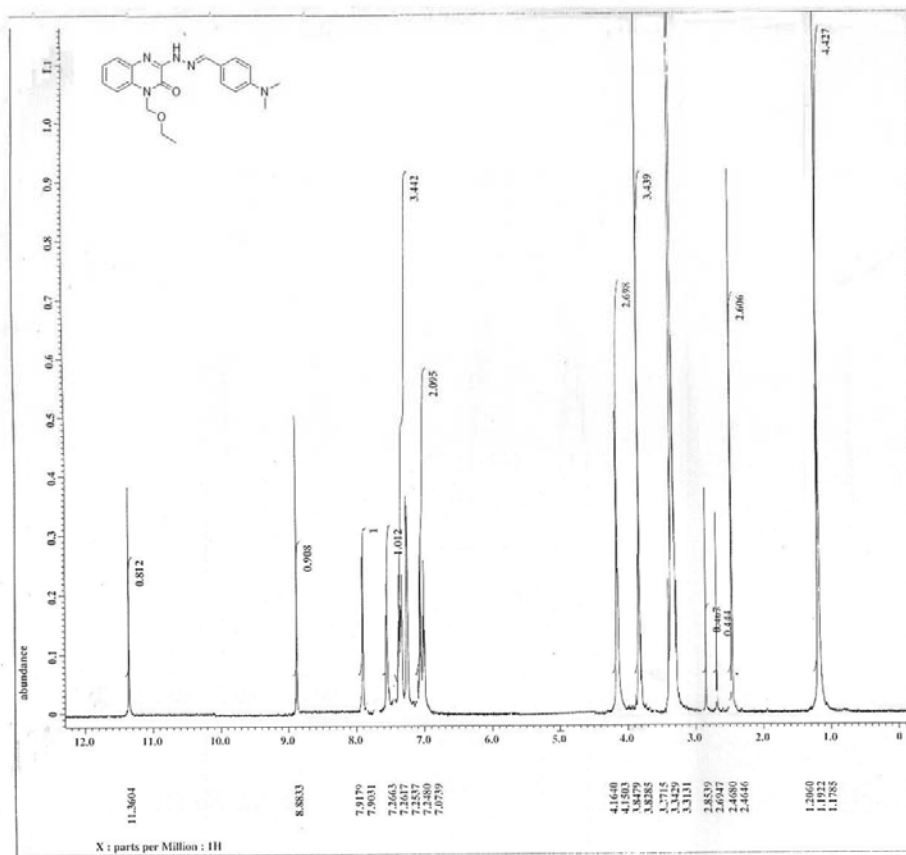
Reagents and conditions:

- i) Diethyl malonate, DMF, Et₃N, reflux, 10 h. ii) Diethyl succinate, DMF, reflux, 12h.

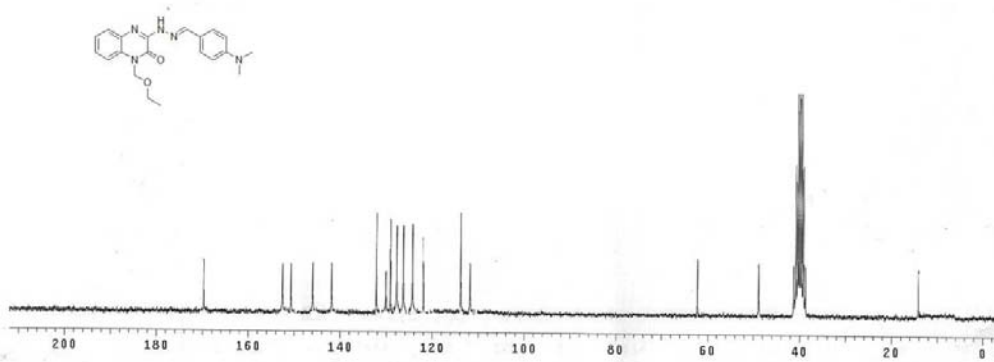
Scheme 5: Synthesis of compounds **19** and **20**

- Synthesis of quinoxaline derivatives **1-20**
- Studying of the possible inhibitory effects of synthesized the quinoxalines on Epstein–Barr virus early antigen activation
- Studying of the inhibition of human tyrosine kinase (TRK)
- Molecular docking study

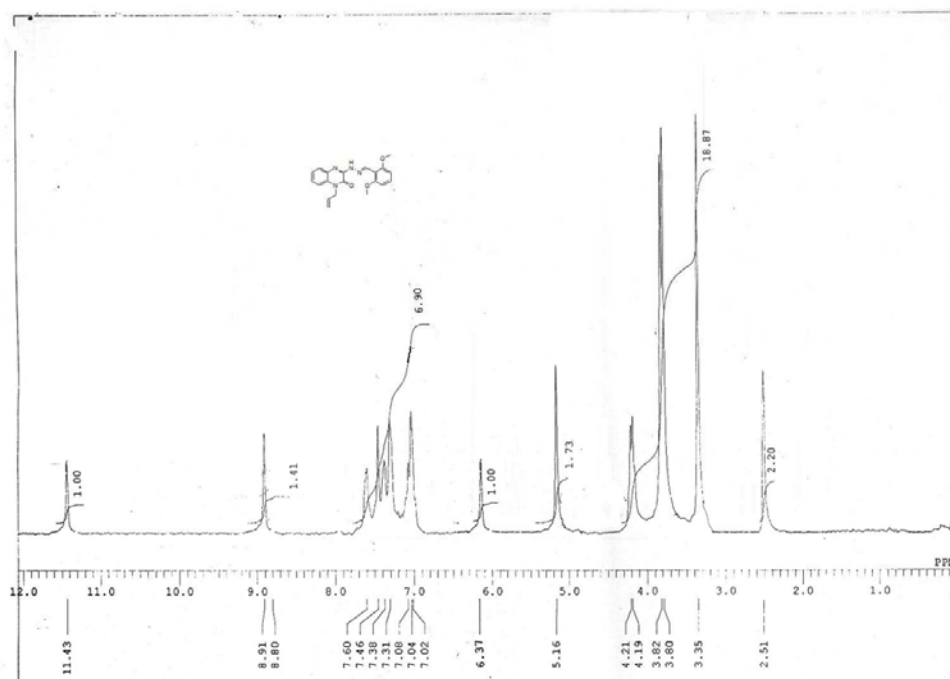
¹H NMR (500 MHz, DMSO-*d*₆) of ethyl 2-(3-(2-(4-(dimethylamino)benzylidene)-hydrazinyl)-2-oxoquinoxalin-1(2*H*)-yl)acetate (8).



^{13}C NMR (500 MHz, $\text{DMSO}-d_6$) of ethyl 2-(3-(2-(4-(dimethylamino)benzylidene)hydrazinyl)-2-oxoquinoxalin-1(2*H*)-yl)acetate (8).

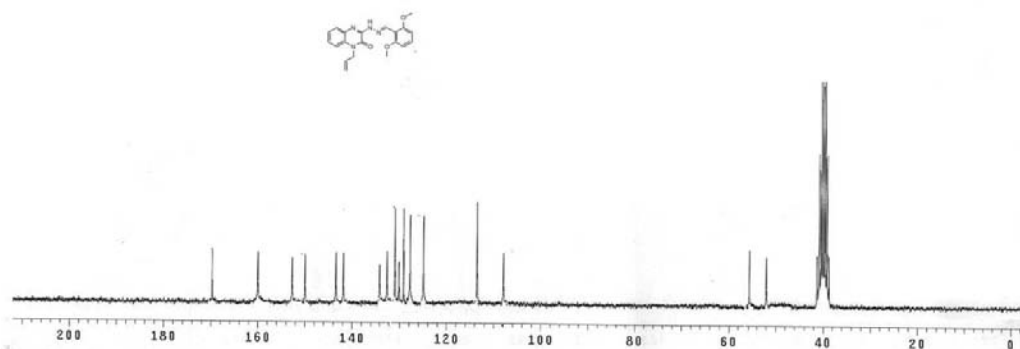


^1H NMR (270MHz, $\text{DMSO}-d_6$) of 1-Allyl-3-(2-(2,6-dimethoxybenzylidene)hydrazinyl)quinoxalin-2(1*H*)-one (9).

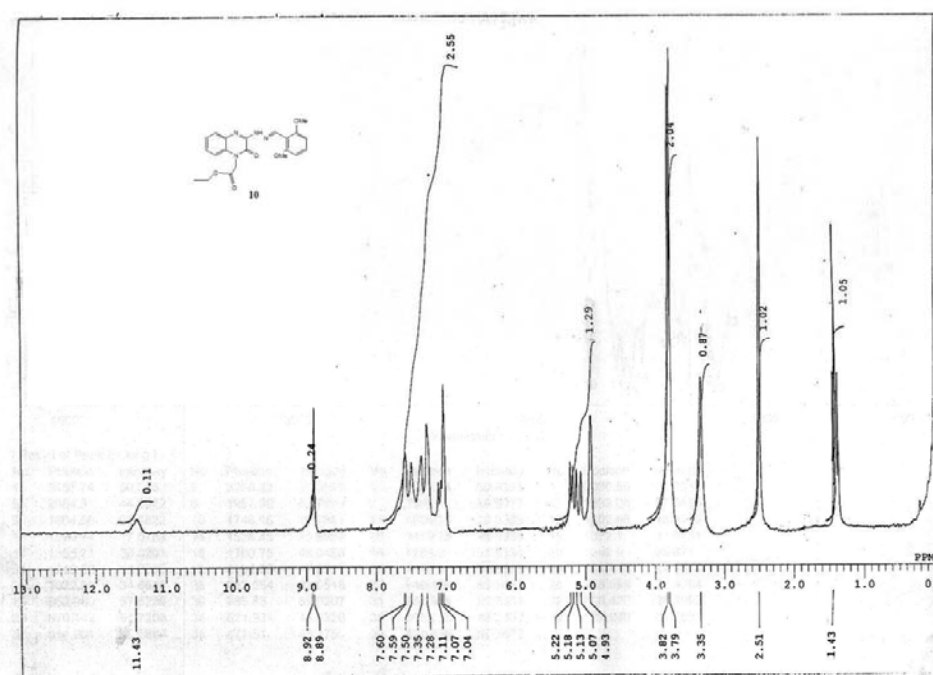


^{13}C NMR (270 MHz, $\text{DMSO}-d_6$) of 1-Allyl-3-(2-(2,6-dimethoxybenzylidene)hydrazinyl)quinoxalin-2(1*H*)-one (9).

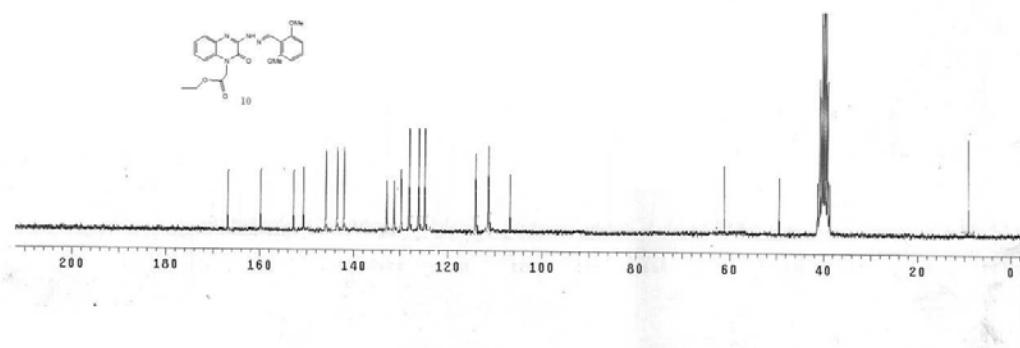
52.5, 55.9, 110.3, 107.8, 113.6, 125.4, 128.1, 129.7, 130.61, 132.7, 134.13, 142.51, 143.5, 150.12, 153.4, 159.8



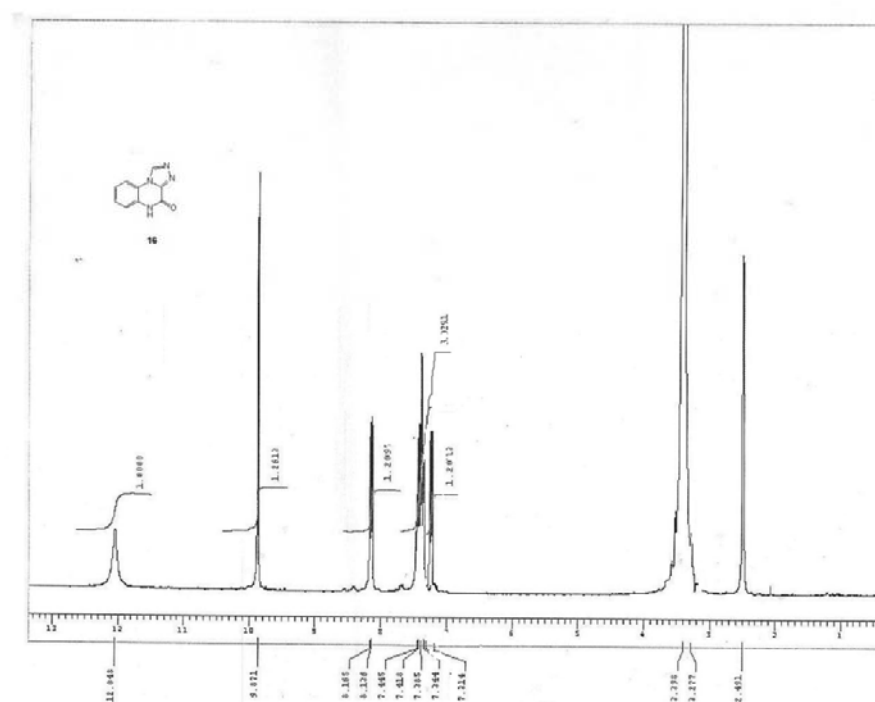
¹H NMR (270 MHz, DMSO-*d*₆) of Ethyl 2-(3-(2-(2,6-dimethoxybenzylidene)hydrazinyl)-2-oxoquinoxalin-1(*2H*)-yl)acetate (10)

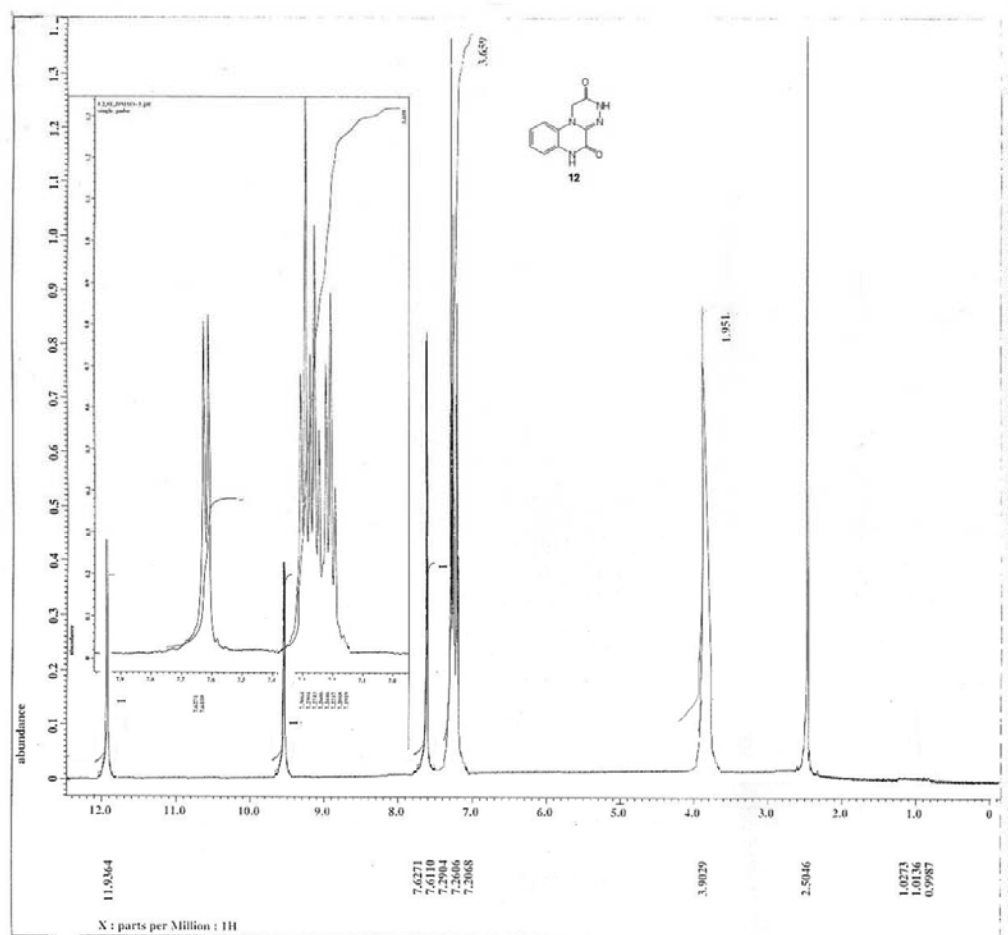


¹³C NMR (270 MHz, DMSO-*d*₆) of Ethyl 2-(3-(2-(2,6-dimethoxybenzylidene)hydrazinyl)-2-oxoquinoxalin-1(*2H*)-yl)acetate (10).:

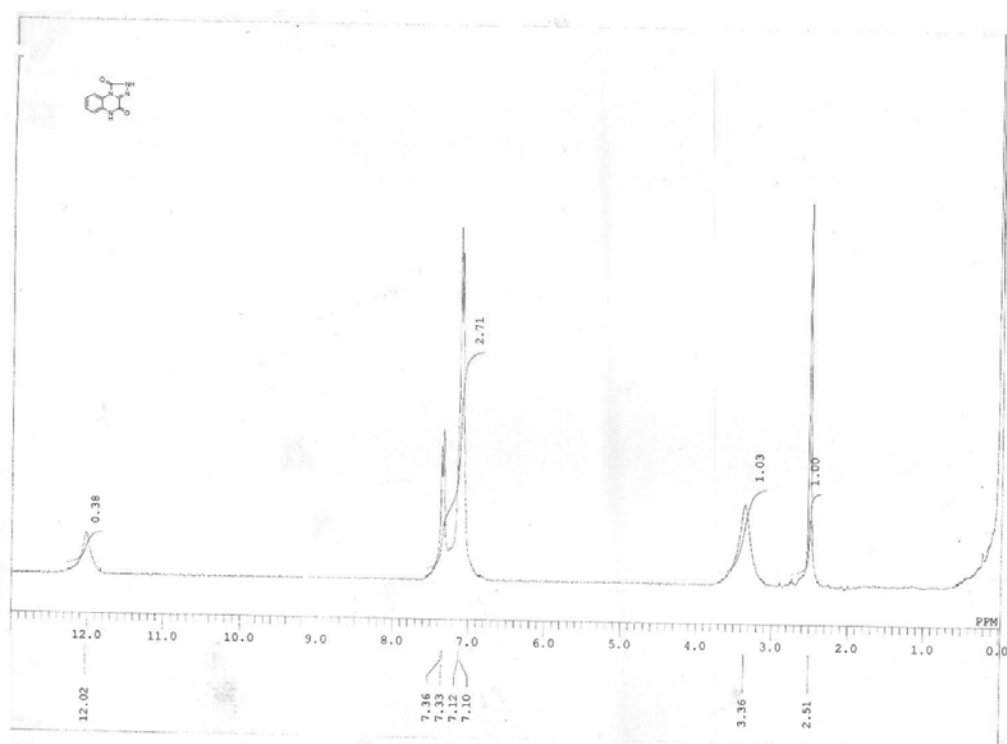


¹H-NMR(270 MHz, DMSO-*d*₆) of [1,2,4]triazolo[4,3-*a*]quinoxalin-4(5*H*)-one (16).

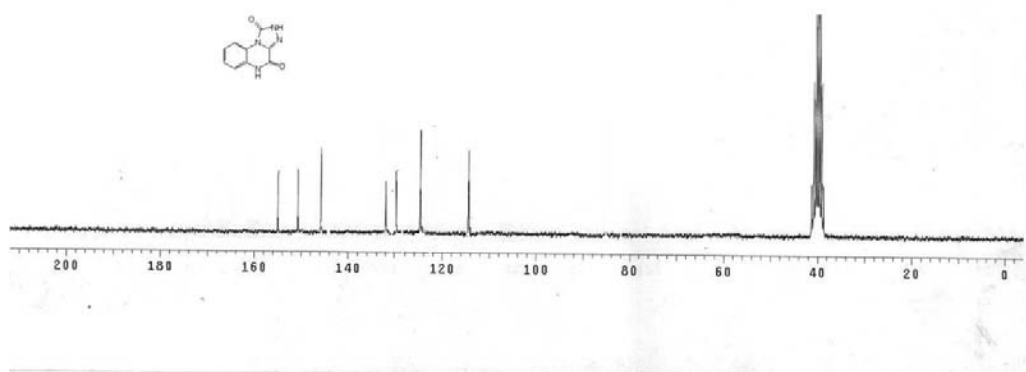




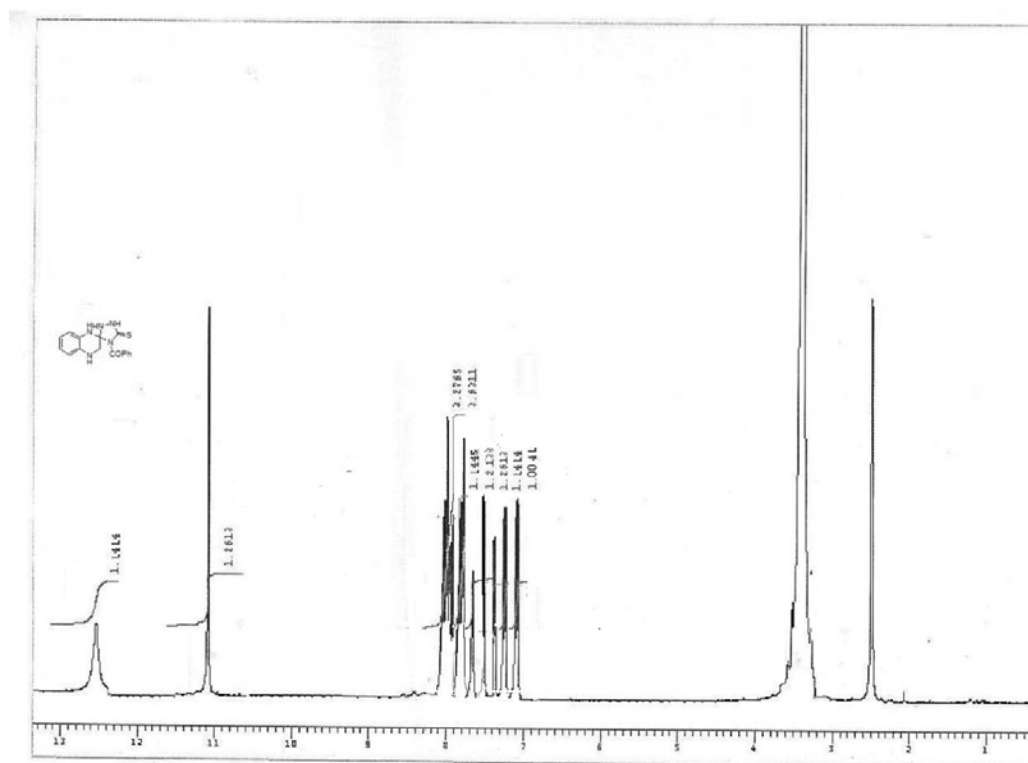
¹H NMR (270 MHz, DMSO-d₆) of [1,2,4]triazolo[4,3-*a*]quinoxaline-1,4(2*H*,5*H*)-dione (15).



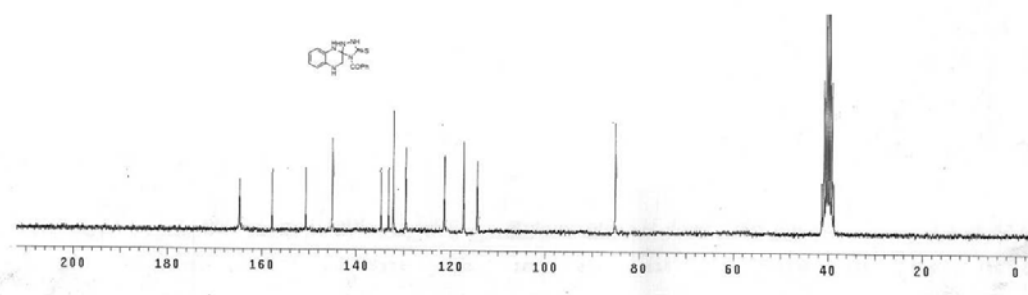
¹³C NMR (270 MHz, DMSO-d₆) of [1,2,4]triazolo[4,3-a]quinoxaline-1,4(2*H*,5*H*)-dione (15).



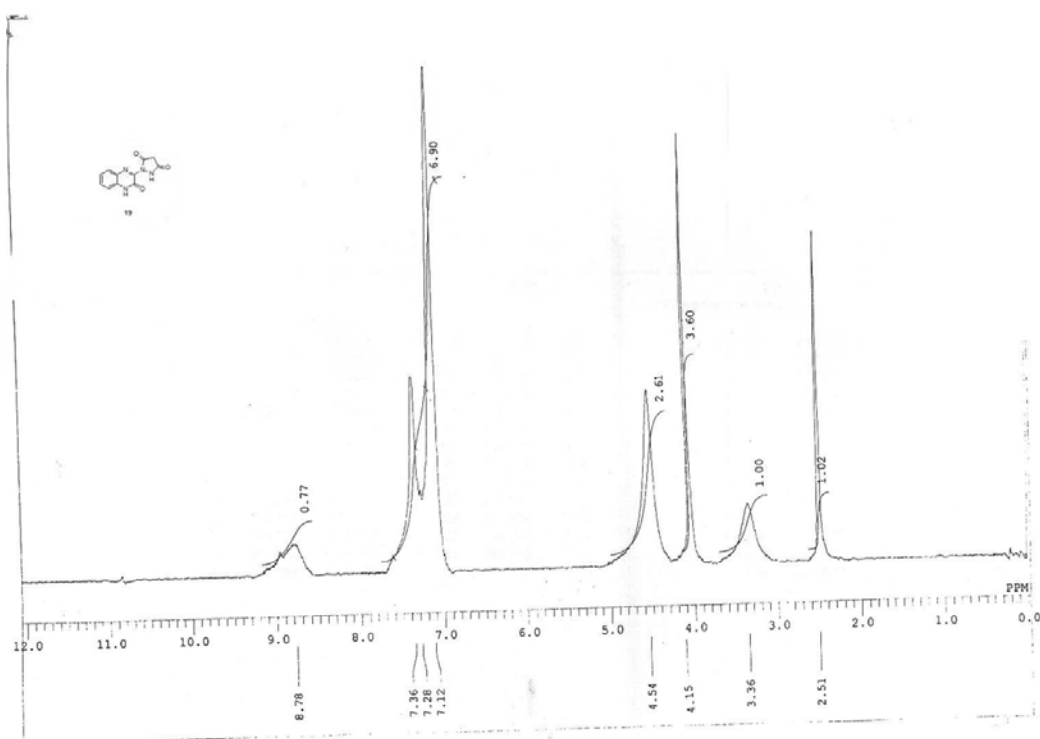
¹H NMR (270 MHz, DMSO-*d*₆) of 4'-Benzoyl-5'-thioxo-1*H*-spiro[quinoxaline-2,3'-[1,2,4]triazolidin]-3(4*H*)-one (18).



¹³C NMR (270 MHz, DMSO-*d*₆) of compound 18



¹H NMR (270 MHz, DMSO-*d*₆) of 1-(3-oxo-3,4-dihydroquinoxalin-2-yl)pyrazolidine-3,5-dione (19)



¹³C NMR (270 MHz, DMSO-*d*₆) of compound 19

